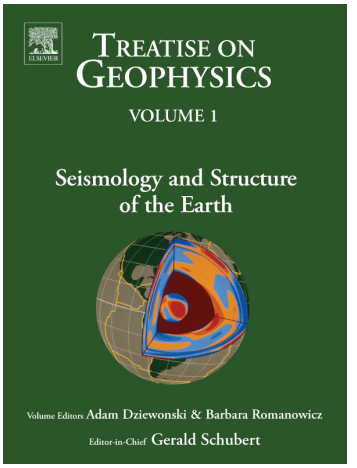

1.21 Deep Earth Structure – *Q* of the Earth from Crust to Core

B. Romanowicz, University of California, Berkeley, CA, USA

B. J. Mitchell, Saint Louis University, St. Louis, MO, USA

1.21.1 Introduction

Seismic waves have long been known to attenuate at a rate greater than that predicted by geometrical spreading of their wave fronts. Knopoff (1964) pointed out more than four decades ago that much of that attenuation must occur because of intrinsic anelastic properties of the Earth. Were it not for that fortunate circumstance, waves generated by all past earthquakes, as noted by Knopoff, would still be reverberating in the Earth today. Since it redistributes rather than absorbs wave energy, scattering would not have the same effect.

A commonly used measure of the efficiency of wave propagation is the quality factor Q or its inverse, the internal friction Q^{-1}. The latter quantity is most often defined by the expression:

$$Q^{-1} = \Delta E/2\pi E_{\max} \qquad [1]$$

where ΔE is the elastic energy lost per cycle and $E_{\max}$ is the maximum elastic energy contained in a cycle. O'Connell and Budiansky (1978) proposed replacing maximum energy by average stored energy in eqn[1], a change that requires the integer 4 replace 2 in that equation. That form of the definition permits writing Q as the ratio of the real to imaginary part of the complex elastic modulus. However, most seismologists use eqn [1].

Because of its strong dependence on temperature, partial melting and water content, mapping anelastic attenuation in the Earth has the potential to provide valuable information on Earth's three-dimensional (3-D) structure and dynamics, in complement to what can be learned from mapping elastic velocities. A significant challenge is to separate the effects of anelastic (or intrinsic) attenuation from those of elastic scattering and focusing due to propagation in elastic 3-D structure.

Practical aspects of seismic-wave attenuation include the need to account for it when determining earthquake magnitudes and when computing realistic synthetic seismograms. In addition, seismologists must know the attenuation structure in the Earth if they wish to determine dispersion that is produced by anelasticity (Jeffreys, 1967; Liu *et al.*, 1976). The principle of causality requires that such velocity dispersion accompany intrinsic attenuation (Lomnitz, 1957; Futterman, 1962; Strick, 1967).

The following sections present a review of our current knowledge about seismic-wave attenuation from earliest studies to the present. It is a rapidly growing field for which measurements have only recently become sufficiently numerous and reliable to allow mapping at relatively small scales. It has consistently been observed that measurement errors are large, and it has recently become clear that systematic, rather than random, errors are the greatest cause of concern in Q determinations.

A major consideration is the frequency dependence of Q. We thus begin by describing the state of understanding of this issue. Next we discuss 1-D models of Q: even now, only the average variation of Q with depth is reasonably constrained in the deep Earth. Following that, we will discuss regional variations of Q in the upper mantle and in the crust, for which robust constraints are beginning to emerge. Earlier reviews on this topic can be found in Mitchell (1995) for the crust, Romanowicz (1998) for the mantle and, most recently, Romanowicz and Durek (2000) for the whole Earth.

1.21.2 Frequency Dependence of Q

Determinations available in the 1960s from seismic observations and laboratory measurements suggested that Q was only weakly dependent on frequency (Knopoff, 1964). That conclusion, however, conflicted with the frequency dependence known for single relaxation mechanisms that exhibit rather narrowly peaked spectra for Q^{-1} centered at a characteristic frequency. Liu *et al.* (1976) reconciled those two observations by considering that, over the seismic frequency band in the Earth, Q^{-1} consists of a superposition of many thermally activated relaxation mechanisms for which maxima occurred at different frequencies. That superposition produces a continuous absorption band with a nearly frequency-independent Q^{-1} distribution in the seismic frequency band (**Figure 1**). The high- and low-frequency limits of the absorption band are described by relaxation times τ_1 and τ_2 and result in the following expression for the absorption band model (Kanamori and Anderson, 1977):

$$Q^{-1}(\omega) = (2/\pi)Q_{\mathrm{m}}^{-1}\tan^{-1}\left[\omega(\tau_1-\tau_2)/\left(1+\omega^2\tau_1\tau_2\right)\right] \qquad [2]$$

where Q_{m} represents the maximum within the absorption band. A more realistic distribution of relaxation times yields a mild frequency dependence $Q \sim \omega^{\alpha}$ within the absorption band (Minster and Anderson, 1981; Mueller, 1986), and $Q^{-1} \sim \omega^{+1}$ at the higher end of the absorption band and $Q^{-1} \sim \omega^{-1}$ at the low end (Minster and Anderson, 1981). Measurements of

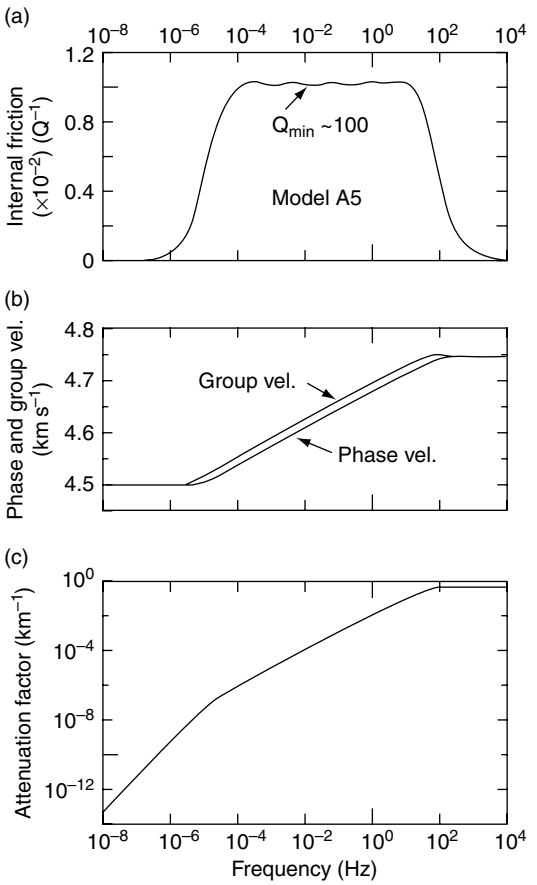

Figure 1 (a) Internal friction (Q^{-1}), (b) phase and group velocity dispersion, and (c) attenuation coefficient as functions of frequency. Reproduced from Liu HP, Anderson DL, and Kanamori H (1976) Velocity dispersion due to anelasticity: Implication for seismology and mantle composition. *Geophysical Journal of the Royal Astronomical Society* 47: 41–58, with permission from Blackwell Publishing.

attenuation of multiple ScS phases (Sipkin and Jordan, 1979) and other body waves (e.g., Sacks, 1980; Lundquist and Cormier, 1980; Der *et al.*, 1982; Ulug and Berckhemer, 1984) have provided evidence that the high frequency corner is located in the band 0.1–1 Hz. A later model (Anderson and Given, 1982) constructed to explain variations of Q for various depths in the Earth from the comparison of surface wave, free oscillation, and body-wave data, obtained a single absorption band with $Q_m = 80$, $\alpha = 0.15$, and a width of five decades centered at different frequencies for different depths in the mantle, with a shift of the absorption band to longer periods at greater depth. Such a model could satisfy many of the known values of Q in the early 1980s. In particular, $\alpha = 0.15$ is compatible with a study of the damping of the Chandler wobble (Smith and Dahlen, 1981).

Many years of body-wave studies have since constrained the frequency dependence $Q \sim \omega^{\alpha}$ in the body-wave band to have $\alpha \sim 0.1$–1. Ulug and Berckhemer (1984) used spectral ratios of S/P waves in the frequency range 0.04–1.5 Hz and found $\alpha \sim 0.25$–0.6. This frequency range was extended to 6 Hz by Cheng and Kennett (2002), who found $\alpha \sim 0.2$–1 in Australia. Flanagan and Wiens (1998) found a factor of 2 difference in Q measured from sS/S and pP/P phase pairs in the Lau backarc region, implying a strong frequency dependence in the 1–10 s period range, and inferred $\alpha \sim 0.1$–0.3.

Recently, Shito *et al.* (2004) used regional waveform data in western Pacific subduction zones to estimate α from P–P spectral ratios in the frequency range 0.08–8 Hz and found a range of $\alpha \sim 0.1$–0.4, which is in agreement with laboratory studies for solid olivine (e.g., Gueguen *et al.*, 1989; Jackson, 2000) and seems to indicate that solid state processes are the primary mechanism for observed attenuation. Indeed, according to laboratory results, partial melting results in weak frequency dependence in a broad frequency range (e.g., Jackson *et al.*, 2004), which is inconsistent with these observations.

In order to reconcile teleseismic S–P differential traveltimes measured by handpicking, on the one hand, and by comparison of observed and synthetic seismograms, on the other, Oki *et al.* (2000) found that a frequency dependence with $\alpha \sim 0.04$ needs to be introduced in the reference PREM Q model (Dziewonski and Anderson, 1981), a value much smaller than in other studies.

At crustal depths, the frequency dependence of Q is usually described by the equation $Q = Q_o f^{\zeta}$ where Q_o is a reference frequency and ζ is the frequency dependence parameter. For shear-wave Q (Q_μ), it appears to be between about 0.0 and 1.0 and varies regionally, with depth in the crust, and with frequency, as will be described in more detail in a later section.

An important consequence of the frequency dependence of Q in the Earth is the presence of velocity dispersion due to attenuation. Velocity dispersion was first recognized to be important when comparing global mantle elastic velocity models based on free oscillation and body-wave traveltime data centered at 1 s. A dispersion correction of 0.5–1.5% helped reconcile these models (Liu *et al.*, 1976; Kanamori and Anderson, 1977) and has been applied systematically in global seismology (e.g., Dziewonski and Anderson, 1981), although Montagner and Kennett (1996) showed that attenuation alone is insufficient to reconcile both types of data and

suggested the need to perturb the density structure and introduce radial anisotropy in different parts of the mantle. In the presence of large lateral variations in Q in the upper mantle, which could be in excess of 100%, it is also necessary to account for velocity dispersion when interpreting global tomographic models in the light of other geophysical data, such as the geoid, as illustrated by Romanowicz (1990) in the case of very long wavelength structure. Karato (1993) estimated the contribution of anelasticity to the calculation of partial derivatives of elastic velocities with temperature, and concluded that it should be important in the deep mantle, as anelastic effects might dominate anharmonic effects at high pressures, a conclusion confirmed by Karato and Karki (2001), who used an improved model for the calculation of anelastic effects, including the nonlinear dependence of attenuation on temperature.

In order to interpret seismologically-derived 1-D and 3-D Q models in the Earth, it is necessary to confront them with laboratory experiments, which should provide constraints on: (1) the physical mechanisms responsible for attenuation (i.e., grain boundary or dislocation processes, (e.g., Jackson, 1993; Karato, 1998)) and the related frequency dependence; (2) the dependence of Q on temperature and pressure. Unfortunately, this has proven to be a major challenge, particularly for the deep mantle, due to the difficulties of reproducing in the laboratory both the high P and high T conditions, the low frequency range of seismic observations, and the location of the absorption band far from the frequency range of ultrasonic experiments, preventing ready extrapolation to seismic frequencies.

The variation of Q_μ with temperature can be expressed as (e.g., Jackson, 1993; Karato, 1993):

$$Q^{-1} = A\omega^{-\alpha}\exp(-\alpha H/RT) \qquad [3]$$

where $H = E^* + PV^*$ is the activation enthalpy, which depends on pressure through the activation volume V^*, a quantity that is not precisely known. One way to circumvent this is to parametrize this expression in terms of homologous temperature T_m/T (e.g., Sato *et al.*, 1989; Karato, 1993; Cammarano *et al.*, 2003):

$$Q^{-1} = A\omega^{-\alpha}\exp(-\alpha g T_m/\mathrm{T}) \qquad [4]$$

where g is a dimensionless factor, which depends on H, the melting temperature T_m and the gas constant R. Such a parametrization removes the need for accurate knowledge of the activation volume, and also allows use of a simple scaling law to relate grain size to frequency (Sato *et al.*, 1989). The pressure dependence is folded into T_m, which is easier to measure in the laboratory.

Much progress in the measurement of attenuation at seismically relevant frequencies has been achieved in the last 15 years (e.g., Jackson, 1993; Karato and Spetzler, 1990; Getting *et al.*, 1997; Faul *et al.*, 2004). Recently, reliable results for olivine have become available at pressures and temperatures down to asthenospheric depths. These advances are described in more detail in Chapter 2.17.

1.21.3 Early Studies

Although seismic-wave attenuation did not become a popular area of research until the 1970s, the first contributions appeared not long after global deployments of seismographs in the early 1900s. Here we describe several important studies completed before 1970, which, in addition to providing the first estimates of Q for several phases, provided the first inklings of the difficulties associated with amplitude measurements.

G. H. Angenheister, working in Göttingen, Germany, in 1906, reported the first known measurements of the attenuation rate of a seismic wave. Instruments at that time were still primitive and surface waves consequently dominated most seismograms recorded by Göttingen's Wiechert seismometers. Angenheister (1906) used records from those instruments to measure the amplitude decay of 20-s surface waves for three different segments of the same great-circle path and found the decay rate to be about $0.000\,25\,\mathrm{km}^{-1}$. For group velocities near $3\,\mathrm{km\,s}^{-1}$ that rate corresponds to a Q value of about 200, a value implying that the measured attenuation coefficient lies within the range of commonly measured 20-s values today. He later published what was probably the first report of regional variations of surface-wave attenuation (Angenheister, 1921) in which he found that the decay of surface-wave amplitudes along oceanic paths was greater than that along continental paths. This result holds only for those cases where attenuation over relatively low-Q oceanic paths is compared to attenuation over high-Q continental paths (Mitchell, 1995).

B. Gutenberg also made some early determinations of Q using surface waves. He determined a Q value of 70 for Love waves at 100-s period (Gutenberg, 1924), and a value of 200 for Rayleigh

waves at 20-s period (Gutenberg, 1945b). The latter value corresponds well with Angenheister's earlier measurement of Rayleigh-wave attenuation at that period. Gutenberg also determined Q for body phases, first finding a Q of 1300 for 4-s P and PKP waves (Gutenberg, 1945a). He then measured Q for three body-wave phases at different periods (Gutenberg, 1958) finding Q's of 2500 for P and PP at 2 s, and 400 for P and PP at 12 s. In the same study he also measured Q for S waves finding values of 700 at 12 s and 400 at 24 s. Press (1956) also determined Q for S waves finding it to be 500 or less.

Evernden (1955) studied the arrival directions of *SV*-, Rayleigh- and Love-wave phases using a tripartite array in California and found that all of those phases deviated from great-circle paths between the events and the array. Although Evernden did not address Q he brought attention to the fact that seismic waves may deviate from a great-circle path during propagation, a problem that continues, to this day, to plague determinations of Q from amplitude measurements.

The 1960s produced the first definitive evidence for lateral variations of body-wave Q even over relatively small distances. Asada and Takano (1963), in a study of the predominant periods of teleseismic phases recorded in Japan, found that those periods differed at two closely spaced stations and attributed that to differences in crustal Q. Ichikawa and Basham (1965) and Utsu (1967), studied spectral amplitudes at 0.5–3.0 Hz frequencies and concluded that P-wave absorption beneath a seismic station at Resolute, Canada was greater than that beneath other stations in northern Canada.

Tryggvason (1965) devised a least-squares method for simultaneously obtaining Rayleigh-wave attenuation coefficients and source amplitudes using several stations located at varying distances from an explosive source. Since he assumed the source radiation pattern in this method to be circular he had no need to determine that pattern or know the crustal velocity structure. In the same year Anderson *et al.* (1965) developed equations that allowed measured surface-wave attenuation to be inverted for models of Q_μ variation with depth and applied it to long-period surface waves that were sensitive to anelasticity at upper mantle depths.

Sutton *et al.* (1967), studied radiation patterns for Pg and Lg phases recorded at several stations in the United States and found that focusing and regional attenuation differences affected both waves. They concluded that the nature of the tectonic provinces traversed by the waves was more important than initial conditions at the source in determining the observed radiation patterns.

1.21.4 1-D Global Mantle *Q* Models

Our knowledge of the 1-D Q structure of the Earth comes primarily from two types of data: normal modes/surface waves on the one hand, multiple ScS on the other. As noted in a previous review of this topic (Romanowicz and Durek, 2000), early studies based on normal mode and surface-wave data developed measurement and inversion methodologies and established the main features of the variation of Q_μ with depth (e.g., Anderson and Archambeau, 1966; Kanamori, 1970; Roult, 1975; Gilbert and Dziewonski, 1975; Jobert and Roult, 1976; Deschamps, 1977; Sailor and Dziewonski, 1978; Buland and Gilbert, 1978; Geller and Stein, 1978). These studies found that:

1. shear-wave attenuation is low in the lithosphere;
2. there is a high attenuation zone roughly corresponding to the low-velocity zone generally associated with the asthenosphere;
3. below 200 km depth, Q_μ increases with depth with a sharp gradient across the transition zone; and
4. Q_μ is higher on average in the lower mantle than in the upper mantle.

Nearly vertically traveling multiple ScS waves provided constraints on the average Q_μ in the whole mantle (e.g., Kovach and Anderson, 1964; Yoshida and Tsujiura, 1975) and confirmed the increase in Q_μ in the mid-mantle. Studies of amplitude ratios of body-wave phases interacting with the core–mantle boundary (CMB) provided early evidence for a possible lower Q_μ zone at the base of the mantle (e.g., Kuster, 1972; Mitchell and Helmberger, 1973). To accommodate both normal mode and body-wave observations, Anderson and Hart (1976, 1978) proposed a model with a Q_μ maximum in the lower mantle, a feature that has successively appeared and disappeared in subsequent whole mantle models based on normal mode and surface-wave data (Masters and Gilbert, 1983; Smith and Masters, 1989; Giardini and Woodhouse, 1988; Li, 1990; Okal and Jo, 2002; Widmer *et al.*, 1991). Some bulk attenuation is necessary to simultaneously fit high Q radial mode data and surface-wave data, and some models such as SL8 (Anderson and Hart, 1978) and the

widely used Preliminary Reference Earth Model (PREM) (Dziewonski and Anderson, 1981) located it in the inner core, while others preferred to place it in the upper mantle (e.g., Sailor and Dziewonski, 1978), and, more recently, in the asthenosphere (Durek and Ekström, 1995).

In the last decade, a problematic discrepancy has emerged between the measurements of fundamental mode Q_R obtained for spheroidal modes using a propagating wave approach (e.g., Dziewonski and Steim, 1982; Romanowicz, 1990, 1994a; Durek *et al.*, 1993; Durek and Ekström, 1996) and those using a standing-wave approach (Smith and Masters, 1989; Widmer *et al.*, 1991; Roult and Clévédé, 2000). In the period band 150–300 s, where measurements by the two methods overlap, Q_R estimates derived from standing-wave observations are systematically higher than those derived from surface waves by about 15–20%, which translates into higher Q_μ in the transition zone for models based on free oscillation data (**Figure 2**). The cause of this discrepancy was first investigated by Durek and Ekström (1997) who explored the influence of realistic background noise on normal mode based measurements, which require the use of long time series. This issue is particularly relevant in the light of the discovery of continuously excited background free oscillations (e.g., Suda *et al.*, 1998). Durek and Ekström (1997) considered several different Q measurement methods: one based on fitting of amplitude or complex spectra, and another classical method based on measuring the decay of the amplitude of a given mode with time. While the background noise does contribute to a bias toward higher Q values, if measurements are done with care, the bias does not exceed about 5–10%, failing to explain the larger observed discrepancy. On the other hand, Masters and Laske (1997) questioned the accuracy of surface-wave Q measurements at very long periods, pointing out the difficulty in finding an appropriate time window isolating the fundamental mode in the presence of overlapping wave trains and overtones. A more recent study by Roult and Clévédé (2000) confirms the higher Q values obtained from mode-based measurements (**Figure 2**). These authors carefully assessed various factors contributing to the uncertainty in mode Q measurements performed using the amplitude decay method, in particular length of time windows for the computation of spectra, and number of time steps for amplitude measurements of individual modes. They also considered the effect of lateral heterogeneity, which they modelled using a higher order perturbation theory that includes multiple scattering

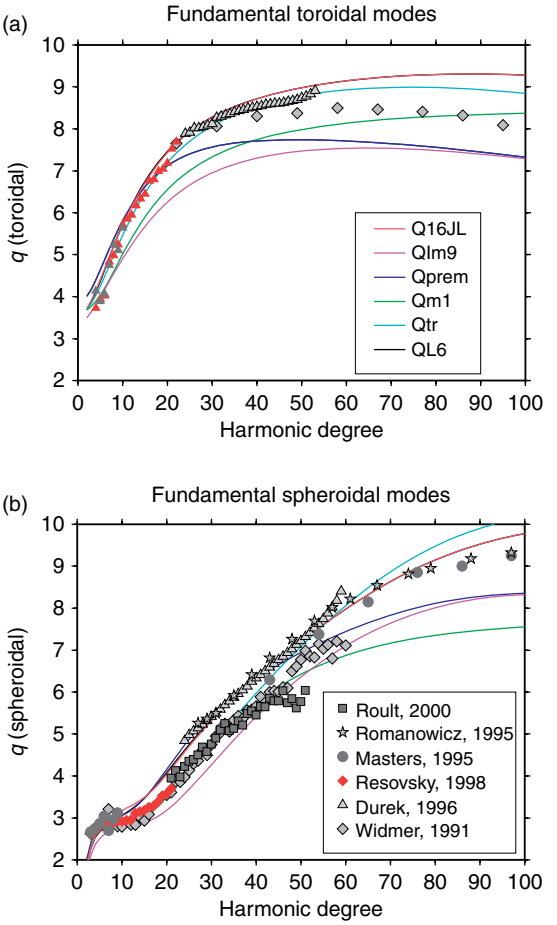

Figure 2 Fundamental mode Q measurements obtained using either a standing mode approach (Widmer *et al.*, 1991; Masters and Laske, 1997; Roult and Clévédé, 2000) or a propagating surface wave approach (Romanowicz, 1995; Durek and Ekström, 1996). Note the discrepancy between the two approaches in the frequency band where both methods can be applied. Also shown are fits to the data for several models of Q_μ shown in **Figure 3**. (a) Toroidal modes, (b) spheroidal modes. Data are from the REM website.

(e.g., Lognonné and Romanowicz, 1990). They concluded that mode Q measurements are more reliable than measurements based on great circle surface-wave amplitude ratios, which they attribute to contamination by higher modes and to the relative deficiency in low frequencies of the first arriving R1 train. We note however that (1) their synthetic tests do indicate some bias toward higher Q's when lateral heterogeneity is added in the normal mode case; (2) their synthetic tests only consider very smooth models of lateral heterogeneity, for which scattering effects are very weak; (3) the QL6 model of Durek and Ekström (1996) was derived from travelling surface-wave data

using a different method than tested by Roult and Clévédé (2000): the method used was a time domain (rather than spectral domain) method where the Q model was derived by estimating the best transfer function from one Rayleigh-wave train to the one that travelled over an additional great circle path. QL6 (**Figures 2** and **3**) not only fits surface-wave data better than mode-based models such as QM1 (Widmer *et al.*, 1991), but it also fits toroidal mode Q data better than both QM1 and PREM (Dziewonski and Anderson, 1981). Therefore, it seems that the question of the mode/surface-wave discrepancy has not been resolved yet. A recent study by Resovsky *et al.* (2005) revisited the construction of a 1-D Q model of the Earth using a forward modelling approach based on the neighborhood algorithm, and produced a family of acceptable models with robust error estimates. Their mode data set was augmented through recent measurements of the attenuation of low angular order modes (e.g., Resovsky and Ritzwoller, 1998; He and Tromp, 1996). They circumvented the mode/surface-wave discrepancy problem by including in their data set both fundamental mode surface-wave and spheroidal mode measurements in the period range 150–300 s, and attributing a low weight to these incompatible data. In some experiments, they even excluded both of these data sets. Their final family of models appears to be in good agreement, on average, with the surface-wave-based model QL6, in particular in the transition zone (**Figure 3**). Resovsky *et al.* (2005) also revisit the question of the location of bulk attenuation in the Earth and find it negligible in the inner core and preferentially located in the outer core and lower mantle.

While PREM and QL6 have constant Q_μ in the lower mantle, the Resovsky *et al.* (2005) study tentatively includes three layers in the lower mantle and confirms the presence of a Q_μ maximum in the mid-lower mantle, as was found in earlier models (SL8, Anderson and Hart; PAR2C, Okal and Jo (2002); QM1, Widmer *et al.* (1991); Q7U15L, Durek and Ekström (1996), see the review by Romanowicz and Durek (2000)). What is perhaps not yet well constrained, is the precise location of this maximum. Recently, Lawrence and Wysession (2006) developed a Q_μ model based on a large global data set of differential ScS/S amplitude measurements, using a niching genetic algorithm to fit the variations of these amplitudes with distance. Because of the nature of their data, their model (QLM9, **Figure 3**) is best constrained in the lower mantle, so they chose to fix the top 400 km of the mantle to the PREM value. The resulting model also provides evidence for the existence of a Q_μ maximum in the lower mantle, in this case right above the D'' region. However, the high Q values which they obtain in

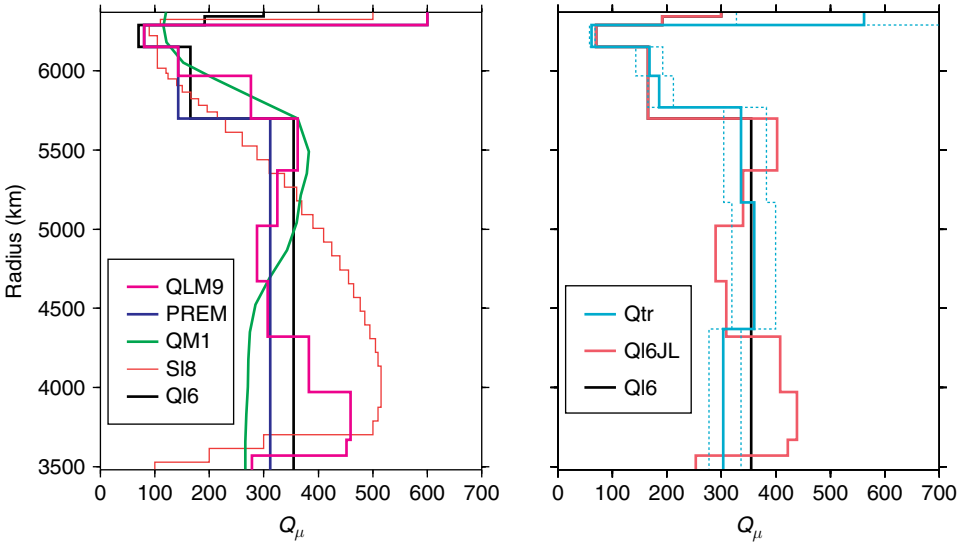

Figure 3 Radial models of Q_μ in the mantle. (Left panel) Models QM1 (Widmer *et al.*, 1991); SL8 (Anderson and Hart, 1978); PREM (Dziewonski and Anderson, 1981); QL6 (Durek and Ekström, 1996); and QLM9 (Lawrence and Wysession, 2006). PREM and QL6 fit fundamental mode Rayleigh wave data, but only QL6 also fits fundamental mode toroidal mode data. Models QLM9 and QM1 have higher Q in the transition zone. Right panel: Qtr: most probable model and 2-sigma standard deviations (broken line) from the work by Resovsky *et al.* (2005), compared to Q16 and a preliminary model which fits both ScS/S amplitude data and fundamental mode surface wave data (Lawrence, personal communication).

the transition zone are incompatible with fundamental mode spheroidal and toroidal data (**Figure 2**, top). Replacing their upper mantle with that of QL6 solves this problem (**Figure 2**, bottom), and little adjustment is needed in the lower mantle to fit the ScS/S amplitude data (Lawrence, personal communication). A joint inversion of mode and ScS/S data sets is underway, and may, in particular, provide some constraints on the frequency dependence of Q_μ as well as shed further light on the surface-wave/mode discrepancy for fundamental modes.

New constraints on average shear and bulk attenuation in the Earth and the core may be forthcoming owing to the high quality digital data set assembled in the last 16 years on the global broadband seismic network, and owing to the occurrence of several very large earthquakes, especially the great Sumatra earthquake of 26 Dec 2004. These data are providing an opportunity to revisit the Q's of the gravest modes of the Earth, in particular the radial mode ${}_0S_0$, and for the first time, measure the Q of individual singlets of modes such as ${}_0S_2$ or ${}_2S_1$ (e.g., Rosat *et al.*, 2005; Roult *et al.*, 2006).

1.21.5 Q in the Core

1.21.5.1 The Outer Core

In the liquid outer core, Q is very high, and generally well approximated by $Q_\kappa \sim \infty$, to fit both free oscillation and body-wave data. Finite Q_κ is, however, required to explain some free oscillation data in the outer core, but the depth range where it is located is still the subject of debate (Anderson and Given, 1982; Widmer *et al.*, 1991; Durek and Ekström, 1996; Resovsky *et al.*, 2005) and, in general, the upper mantle and/or the inner core are preferred locations for finite Q_κ. Likewise, while some evidence for finite Q_κ from short period core phases has been suggested, it is not clear that it is resolvable (Cormier and Richards, 1976).

1.21.5.2 Attenuation in the Inner Core

Attenuation in the inner core is investigated using inner core sensitive modes, as well as spectral amplitude ratios of different core phases. Topics that have been the subject of recent work include

- the comapatibility of normal mode and body-wave measurements, and implications for the frequency dependence of Q in the inner core;
- variations with depth;
- anisotropy; and
- hemispherical variations at the top of the inner core.

From early on, measurements of amplitude ratios of PKP(DF) (sampling the inner core) and PKP(BC) (sampling the outer core) constrained Q_α in the top 500 km of the inner core to be in the range 200–600 (e.g., Sacks, 1969; Doornbos, 1974; Bolt, 1977; Cormier, 1981; Doornbos, 1983; Choy and Cormier, 1983; Niazi and Johnson, 1992; Bhattacharyya *et al.*, 1993; Song and Helmberger, 1993; Tseng *et al.*, 2001; Ivan *et al.*, 2005) and most studies have suggested an increase of Q_α with depth. Others have suggested that Q_α is constant with depth (e.g., Niazi and Johnson, 1992; Bhattacharyya *et al.*, 1993). In these studies, the sampling depth range was limited by the narrow distance range in which the phase PKP(BC) is observed. Extending the depth range sampled by previous studies to 600 km by including diffracted PKP(BC) phases, Souriau and Roudil (1995) proposed a two-layered model with $Q_\alpha \sim 200$ in the topmost 100 km of the inner core, and $Q_\alpha \sim 440$ below. Cormier *et al.* (1998) designed a new approach that allowed them to investigate the variation of Q_α deeper in the inner core, by comparing observed and synthetic PKIKP waveforms in the distance range 150–180°. The synthetic waveforms are built using the source time history of each earthquake, determined from the analysis of P waveforms, and include the effects of mantle attenuation. In a recent improved implementation of this method, which takes into account surface reflections and reverberations near the source, Li and Cormier (2002) obtained a mean for the inner core of Q_α 307 ± 90 and much stronger attenuation in the top 300 km of the inner core. Testing the hypothesis of an innermost inner core, Cormier and Stroujkova (2006) found a rapid change in the magnitude and variance of seismic attenuation of PKIKP in the middle of the inner core, in the interval 400–600 km in Earth radius (**Figure 4**).

Normal modes primarily provide constraints on Q_β, and Q_β and Q_α are related through (Anderson and Hart (1978)):

$$Q_\alpha^{-1} = \frac{4}{3}(V_S/V_P)^2 Q_\beta^{-1} + \left[1 - \frac{4}{3}(V_S/V_P)^2\right] Q_\kappa^{-1} \quad [5]$$

If there was no significant attenuation in bulk, and no frequency dependence, the inferred Q_β from body-wave studies would be on the order of ~ 40. Confronting this value with measurements based on

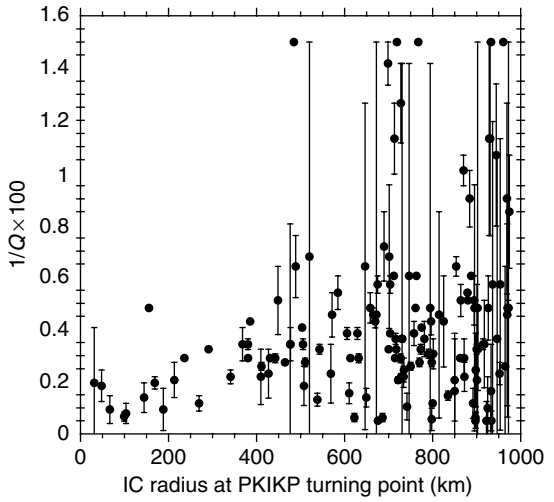

Figure 4 Observed attenuation of PKP(DF) waves as a function of the turning radius of the ray. Reproduced from Cormier VF and Stroujkova A (2006) Waveform search for the innermost inner core. *Earth and Planetary Science Letters* 236: 96–105.

inner core sensitive normal mode data has resulted in some puzzles. Early normal mode studies found very large values of Q_μ (1500–3500) based on the measurement of attenuation of spheroidal core modes (Buland and Gilbert, 1978; Masters and Gilbert, 1981) whereas most more recent models have much lower Q_μ, such as PREM ($Q_\mu = 85$ (Dziewonski and Anderson, 1981), or QM1 ($Q_\mu = 110$, (Widmer *et al.*, 1991)), which is also compatible with measurements of Giardini and Woodhouse (1988). On the other hand, applying the Sompi method (Kumazawa *et al.*, 1990), Suda and Fukao (1990) measured Q_μ of modes sensitive to shear in the top part of the inner core and found very large values and an increase with depth, with $Q_\mu = 1500$ in the top 200 km and $Q_\mu = 3800$ at greater depth. However, their identification of modes has been questioned and, recently, Andrews *et al.* (2006) have shown that measurements of inner core Q_μ could be biased by neglecting mode coupling. Through the comparison of observations and synthetic predictions including mode coupling effects, these authors found that models with very high Q_μ are incompatible with the observations, which favor moderate values of $Q_\mu \sim 80$–100. While such moderate values are now established in the top part of the inner core, where normal modes concentrate their sensitivity, a recent observation of PKJKP, which samples deep into the inner core (Cao *et al.*, 2005), has provided the opportunity to estimate the average Q_μ in the inner core, which was found to be >150 (Cao, 2005), and which would imply an increase with depth, like that for Q_α. This result, however, needs to be confirmed by additional observations of PKJKP.

Even the lowest proposed values for Q_μ currently favored are incompatible with the Q_α results, unless one invokes either: (1) significant bulk attenuation in the inner core or, (2) significant frequency dependence of Q or, (3) a significant scattering component. The rather low value for Q_α found is compatible with the existence of a mushy zone in the top part of the inner core, whose presence is related to the process of solidification of iron alloy (Loper and Roberts, 1981; Fearn *et al.*, 1981; Loper and Fean, 1983) involving a solid matrix and fluid inclusions. This would result primarily in compressional attenuation and could explain some of the observations of seismic anisotropy in the inner core (e.g., Singh *et al.*, 2000). Bowers (2000) cautioned that the large scatter observed in Q_α measurements from PKP amplitude ratios could be due to the effects of lateral variations in structure near the CMB, and in particular the presence of ultralow velocity zones. On the other hand, Krasnoshchekov *et al.* (2005) suggested that variability in the amplitudes of inner core boundary (ICB) reflected PKiKP phases could be due to a mosaic of partially molten patches of scale length 10–100 km.

1.21.5.2.1 Hemispherical variations

Another observation in favor of the presence of a mushy transition zone at the top of the inner core is that of hemispherical differences, first observed in elastic velocity using differential traveltime measurements of the pair of phases PKiKP, postcritically reflected at the ICB and PKIKP, which, in the distance range 120–144° samples the top ~100 km of the inner core (Tanaka and Hamaguchi, 1997; Creager, 1999; Niu and Wen, 2001; Garcia, 2002). These phases have almost the same ray paths in the mantle and in the outer core, so the differences in traveltimes and amplitudes can be attributed to the vicinity of the ICB. Indeed, in a study covering the epicentral distance range 131–141°, the faster eastern hemisphere (40° E to 180° E was also found to have lower Q than the slower western hemisphere (Wen and Niu, 2002). In order to better constrain the depth dependence of the hemispherical variations in Q, Cao and Romanowicz (2004) extended the epicentral distance range to 144°, and found large differences in Q_α, with $Q_\alpha \sim 335$ in the western hemisphere and ~160 in the eastern hemisphere, which they interpreted as resulting from small lateral temperature variations at the top of the inner core. Such

temperature variations could be imposed on the inner core by heterogeneities at the CMB (e.g., Sumita and Olson, 1999) and would influence the connectivity of fluid inclusions in the mushy zone. Below about 85 km depth the hemispherical differences appeared to wane. However, several studies found evidence for persisting differences at greater depth. Oreshin and Vinnik (2004) measured spectral ratios of PKP(DF) and either PKP(AB) or PKP(BC) in the distance range 150–170° and found differences in Q between the hemispheres to a distance of 155°. Yu and Wen (2006) combined observations of PKiKP/PKIKP in the distance range 120–141° and PKP(BC)/PKIKP in the distance range 146–160°, along equatorial paths and proposed that they could resolve hemispherical differences in Q down to at least 200 km (**Figure 5**). However, in the distance range 149–155°, PKP(BC) interferes with PKiKP, causing large scatter in the data. On the other hand, Li and Cormier (2002) did not find evidence for such hemispherical variations in the deeper inner core using PKIKP data at larger distances.

1.21.5.2.2 Anisotropic attenuation

The presence of velocity anisotropy is well documented for the inner core (e.g., Morelli *et al.*, 1986; Woodhouse and Wong, 1986; Creager, 1992; Shearer, 1994; Vinnik *et al.*, 1994; Su and Dziewonski, 1990). Theoretical studies indicate that anisotropy in attenuation should accompany anisotropy in velocity, and several authors have noted the stronger attenuation of PKP(DF) phases travelling along polar paths (Creager, 1992; Song and Helmberger, 1993). Souriau and Romanowicz (1996) examined a carefully selected data set of PKP(DF)/PKP(BC) amplitude ratios for paths whose turning points were located under western Africa, and for which good azimuthal coverage was available. They found a significant correlation between high attenuation and high velocity and inferred that the origin of anisotropy in the top half of the inner core must be due to the orientation of iron crystals, which would produce this type of correlation (Carcione and Cavallini, 1995) rather than fluid inclusions, which would result in correlation of high velocity with low attenuation (Peacock and Hudson, 1990). These results were subsequently extended to a global data set (Souriau and Romanowicz, 1997) and to antipodal paths (Cormier *et al.*, 1998). The latter result was confirmed by Li and Cormier (2002) who suggested that anisotropy in attenuation also varies with depth. As will be seen below, these authors' preferred interpretation involves scattering. Oreshin and Vinnik (2004) confirmed the correlation of anisotropy in attenuation with that in velocity, which, however, may not be present at high latitudes (Helffrich *et al.* (2002)).

1.21.5.2.3 Causes for attenuation in the inner core

In a series of papers, Cormier and collaborators recently explored two different interpretations for the attenuation in the inner core, invoking a viscoelastic and scattering mechanism, respectively (Cormier *et al.*, 1998; Li and Cormier, 2002; Cormier and Li, 2002). In the viscoelastic interpretation, they considered the absorption band model of Cormier and Richards (1988) and, through a parameter search approach, sought to constrain the low frequency corner τ_1, as well as the peak attenuation Q_m^{-1} and the attenuation at 1 Hz (Li and Cormier, 2002). While constraining τ_1 turned out to be problematic, they found that the data are consistent with frequency dependent attenuation in the inner core and weak velocity dispersion in the seismic body-wave band. The existence of scattering, at least at the top of the inner core, was clearly documented by Vidale and Earle (2000) through the modeling of PKiKP coda. In the scattering interpretation, Cormier and Li (2002) investigated a model of inner core attenuation due to forward scattering by 3-D fabric caused by solidification texturing, which could also be responsible for the observed depth-dependent inner core anisotropy. They found a mean scale length of heterogeneity of 9.8 ± 2.4 km and a mean velocity perturbation of $8.4 \pm 1.8\%$. They confirmed the depth dependence found in the viscoelastic interpretation, but with a sharper transition between the highly attenuating upper part of the inner core and the lower attenuating center (e.g., **Figure 5**). They suggested that scattering plays a dominant role in attenuating inner core traversing phases in the frequency band 0.02–2 Hz, as it can also explain elastic and anelastic anisotropy and their depth dependence and helps reconcile the body wave and normal mode Q measurements.

1.21.6 Global 3-D Attenuation Structure in the Upper Mantle

1.21.6.1 Normal Modes and Long Period Surface Waves

1.21.6.1.1 Early studies

In the 1970s, after the occurrence of the 1960 Great Chile Earthquake (Mw 9.6), and with the accumulation of data from the World-Wide Standardized

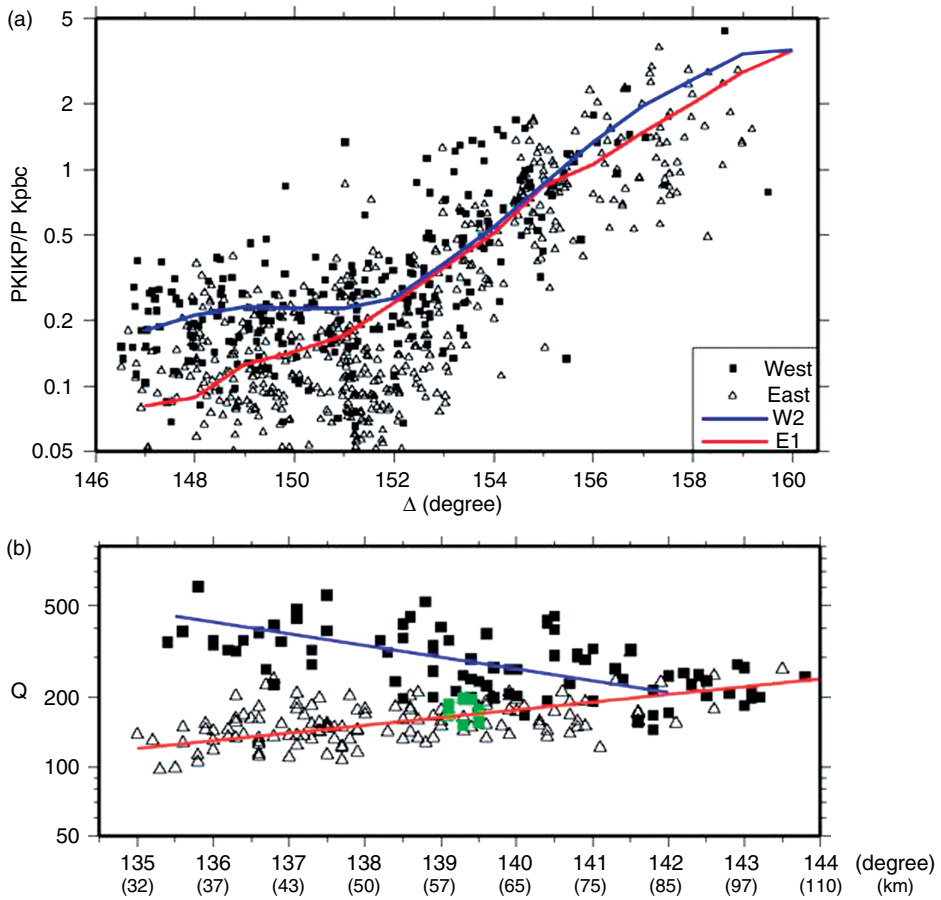

Figure 5 Hemispherical variations of *Q* in the inner core. (a) Variations of amplitude ratios of PKIKP/PKP(BC) as a function of distance and predictions of *Q* models for the western (W2) and eastern (E1) hemispheres. (Adapted from Yu W and Wen L (2006) Seismic velocity and attenuation structures in the top 400 km of the Earth's inner core along equatorial paths. *Journal of Geophysical Research* 111: (doi:10.1029/2005JB003,995). (b) *Q* measurements as a function of distance from amplitude ratios of PKIKP/PKiKP showing differences between the western (triangles) and eastern (squares) hemispheres. From Cao A and Romanowicz B (2004) Hemispherical transition of seismic attenuation at the top of the Earth's inner core. *Earth and Planetary Science Letters* 228: 243–253.

Seismographic Network (WWSSN) network, measurements of long-period surface-wave attenuation, then based on relatively few records, showed large disagreements (e.g., Ben-Menahem, 1965; Smith, 1972; Mills and Hales, 1978; Jobert and Roult, 1976). At that time it was realized that: (1) elastic effects were important in limiting the accuracy of Q measurements; (2) anelastic attenuation caused frequency dependence of elastic velocities, which needed to be taken into account (Luh, 1974; Randall, 1976; Liu *et al.*, 1976; Akopyan *et al.*, 1976; Kanamori and Anderson, 1977); and (3) large systematic lateral variations existed, correlated with those of phase velocities and suggesting significant differences in attenuation under different tectonic regions, with low attenuation under shields and high attenuation under oceans and tectonically active provinces (e.g., Nakanishi, 1978, 1979b, 1981; Lee and Solomon, 1979; Roult, 1982; Dziewonski and Steim, 1982).

While most upper mantle 3-D Q models up to now, as we will discuss below, have been on surface waveform or amplitude data, several authors attempted to measure lateral variations in Q from normal mode data, which in principle should provide sensitivity at greater depths in the mantle. Because the mode amplitude data set is very contaminated by elastic effects (e.g., Smith and Masters, 1989) it was possible to recover only the longest wavelengths in the even degree structure (Romanowicz *et al.*, 1987; Roult *et al.*, 1984; Suda *et al.*, 1991). The most important result of these early studies is the presence of a long wavelength, degree two, structure in Q_μ in the transition zone, shifted toward

the west with respect to the degree two in the shallower mantle, with lowest Q centered in the central Pacific Ocean and under Africa.

1.21.6.1.2 Anelasticity and focusing

One of the main issues limiting resolution in global mantle attenuation tomography is the contamination of amplitudes by elastic focusing effects. Numerous cases of such contamination in Earth circling mantle waves have been reported. For example, for moderate size earthquakes, for which the effect of source directivity can be ruled out, one expects successive Rayleigh-wave trains to gradually decrease in amplitude, due to the effects of attenuation and geometrical spreading. However, it is sometimes observed that an R_{n+1} train has larger amplitude than R_n, where n is the orbit number of the Rayleigh wave (e.g., Lay and Kanamori, 1985; Romanowicz, 1987, 2002), and such observations can be qualitatively reproduced by including focusing effects in synthetic seismograms obtained by normal mode summation (e.g., Romanowicz, 1987). Also in the frequency domain, long-period surface-wave amplitude spectra are often irregular, with many 'holes' that cannot be attributed to intrinsic attenuation or source effects (e.g., Romanowicz, 1994a).

To first order, in the framework of single scattering and in the high frequency approximation, analytical expressions have been obtained for the focusing effect, both in a propagating wave formalism (Woodhouse and Wong, 1986) and in a normal mode asymptotic formalism (Romanowicz, 1987; Park, 1987). Using asymptotic approximations in the framework of normal mode theory, it was shown that focusing effects depend on the transverse gradients of elastic structure, as expressed in terms of phase velocity perturbations in the case of propagating waves, and of local frequency perturbations, in the case of normal modes. The expressions obtained in both approaches are equivalent (Romanowicz, 1987). In the propagating surface-wave case and in the frequency domain,

$$\ln \delta A_F(\omega) = \frac{1}{2}\operatorname{cosec}\Delta \int_0^{\Delta} [\sin(\Delta-\phi)\ \sin\ \phi\partial_\theta^2 - \cos(\Delta-2\phi)\partial_\phi]\frac{\delta c}{c_0}(\omega)\mathrm{d}\phi \quad [6]$$

where Δ is epicentral distance, ϕ is the angular distance along the source-station great circle path, $\delta c/c_0$ is the relative perturbation in phase velocity along the path, and $\delta A_F(\omega)$ is the contribution to the amplitude at frequency ω due to focusing.

In the standing-wave case and time domain, for an isotropic source:

$$\delta F_K(\Delta) = \frac{a\Delta}{U}\left(\frac{\hat{D}_K - \tilde{D}_K}{2k} + \frac{\cot\Delta}{8k}(\delta\hat{\omega} - \delta\tilde{\omega})\right) \quad [7]$$

where $F = (1 + \delta F_K(\Delta))$ is the perturbation to the time domain amplitude of the seismogram for multiplet K, $\delta\hat{\omega}$ and $\delta\tilde{\omega}$ are the perturbations to the great circle average and minor are average local frequencies, respectively, $k = l + 1/2$ where l is the angular order of the mode, and we have defined

$$\tilde{D} = \frac{1}{\Delta}\int_0^{\Delta} \partial_T(\delta\omega_K(s))\mathrm{d}s$$
$$\hat{D} = \frac{1}{\Delta}\int_0^{2\pi} \partial_T(\delta\omega_K(s))\mathrm{d}s \quad [8]$$

where ∂_T denotes the second transverse derivative along the great circle path, which reduces to the integrand in eqn [6]. Accounting for the radiation pattern in eqns [7] is equivalent to using eqns [6] together with ray tracing.

Because the focusing effects are so strongly dependent on the transverse gradients of the elastic structure, and because those are not generally well constrained, compounded by the fact that these expressions are approximate and valid only to first order, it has been a difficult challenge, for the last decade, to properly account for focusing effects in surface-wave attenuation tomography. Indeed, if the corrections made on the basis of an existing elastic model are inaccurate, they can potentially introduce more biases than they can correct.

Noting that focusing effects and attenuation behave very differently as Rayleigh waves circle around the Earth, with the sign of attenuation always the same, while focusing/defocusing depends on the direction of propagation along the great circle, Romanowicz (1990) and Durek *et al.* (1993) showed that, by using four consecutive Rayleigh-wave trains, one can eliminate, at least in the first order approximation, the effect of focusing, as well as uncertainties in the source amplitude. This resulted in the first, low degree, even degree global tomographic models of attenuation in the upper mantle which confirmed the existence of a strong degree 2 in attenuation, as first suggested in studies based on normal modes. These models showed that attenuation in the uppermost mantle was correlated with seismic velocities, at least at the longest wavelengths (~4000 km). There are two drawbacks to this approach: first, only even degree structure can be retrieved in this fashion, as only great-circle average attenuation can be measured. Second, elastic

effects become increasingly more pronounced as distance increases, and the first order approximation is not suitable for higher orbit trains, leading to a decrease in the ability to retrieve the intrinsic attenuation signal. Moreover, higher orbit trains are more dispersed, limiting the frequency range in which Rayleigh waves of consecutive trains do not interfere with each other and/or with overtones.

In order to be able to retrieve odd degree structure while not explicitly correcting for unknown focusing effects, and avoiding the drawbacks of using multiple orbit wave trains, a different approach was proposed by Romanowicz (1995), using three consecutive Rayleigh wave trains (R1, R2, R3). She noted that the R1 and R2 trains are the least contaminated by focusing effects. However, their amplitudes also depend on uncertainties in the source amplitude. The source amplitude shift varies slowly with frequency, and can be estimated by comparing the overall level of the amplitude spectrum computed in two different fashions: (1) directly from R1 (or R2) and (2) using a linear combination of R1, R2, and R3. Romanowicz (1994a) measured attenuation coefficients on R1 and R2 wave trains, correcting for the source shift using the reference provided by the R1, R2, R3 combination. This, combined with a rigorous data selection in which all R1 and R2 amplitude spectra that were not smoothly varying with frequency were rejected, led to the first low degree (equivalent to about degree 5) tomographic model of upper mantle shear attenuation, *QR*19 (Romanowicz, 1995). Even though this first model had very low resolution, it confirmed the correlation of lateral variations of Q with V_S in the top 250 km of the upper mantle, and a shift to a different pattern in the transition zone, dominated by low Q in the central Pacific and Africa, and correlated with hotspots. Romanowicz (1994b) showed that, in the transition zone, at least at the longest wavelengths, anelastic attenuation correlated with the hotspot distribution, whereas the velocity structure correlates better with the slab distribution, consistent with expectations that Q is more sensitive to high temperature regions. The desensitizing approach used, however, limited the lateral resolution of the model obtained, since a relatively small number of paths qualified for inclusion in the inversion.

The applicability of the linear asymptotic approximation to the computation of focusing (eqns [6]–[9]) has been tested by Selby and Woodhouse (2000) on a large data set of Rayleigh-wave amplitudes on minor and major arcs, in the period range 73–171 s. These authors derived maps of lateral variations of $q_R(\omega) = Q_R^{-1}(\omega)$ at different frequencies, assuming that the amplitude of a fundamental mode Rayleigh wave observed at distance Δ and angular frequency ω can be written as:

$$A(\omega, \Delta) = A_0(\omega)(1 + F(\omega))\exp[-\omega a \Delta \bar{q}_R(\omega)]/2U_0(\omega) \quad [9]$$

where U_0 is group velocity, a is the radius of the earth, $A_0(\omega)$ is source term, and $\bar{q}_R(\omega)$ is the average Rayleigh-wave attenuation along the source station path:

$$\bar{q}_R(\omega) = \frac{1}{\Delta}\int_0^{\Delta} q_R(\omega, \theta, \phi)\mathrm{d}s \quad [10]$$

$F(\omega)$ represents the effect of focusing, which can be calculated from a reference elastic 3-D model using expression [6]. Selby and Woodhouse (2000) compared the maps obtained by: (1) inverting the observed amplitude data set for lateral variations in q_R without correcting for focusing, (2) inverting synthetic maps of apparent attenuation obtained by assuming the amplitudes are only affected by focusing and using the elastic phase velocity model of Trampert and Woodhouse (1995), and (3) inverting the observed amplitude data set for q_R after correcting for focusing. In these experiments, a degree 20 model of 3-D apparent attenuation was obtained. They concluded that at the longer periods (e.g., 146 s), the apparent attenuation maps obtained in (2) were not significantly correlated with those obtained in (1), indicating that the amplitude signal is not severely affected by focusing, whereas at the shorter periods (e.g., 73 s), the correlation is stronger. This implies not only that the shorter period data need to be corrected for focusing before inferring lateral variations in intrinsic attenuation, but that the predictions from existing elastic models using the approximate focusing theory were perhaps of practical use, even though these focusing terms depend strongly on the poorly constrained transverse gradients of the elastic structure. Also, Selby and Woodhouse (2000) found that low degree attenuation structure (up to degree 8 in a spherical harmonics expansion) is not significantly affected by focusing in the entire period range considered. In a subsequent study, they inverted the maps of $q_R(\omega)$ with and without corrections for focusing to obtain a series of models of lateral variations of attenuation in the upper mantle up to degree 8 (Selby and Woodhouse, 2002). In the latter study, they also considered the effect of uncertainties in the source term, and found that a frequency dependent correction factor is necessary to combine the $q_R(\omega)$ maps into a successful depth dependent

model of attenuation. They concluded that the details of focusing and source corrections did not affect the robustness of their models up to degree 8, but would be more important at shorter wavelengths.

1.21.6.1.3 Current status

An important result of the Selby and Woodhouse studies was the confirmation that surface-wave amplitudes contained information not only on anelastic structure but also on elastic structure, that could be exploited, as already suggested by Woodhouse and Wong (1986) and Wong (1989). At about the same time, Billien and Lévêque (2000) made the first attempt at inverting simultaneously Rayleigh-wave amplitude and phase data, for maps of phase velocity and q_R between 40–150 s. The effects of focusing were included using eqn [6] which allowed them to consider shorter periods and shorter wavelengths. The maps obtained at short periods indicate significant correlation between phase velocity and attenuation, and therefore tectonics, and the even degree part (degrees 2, 4, 6) of their longer period maps are compatible with those of other studies. However, their odd degree part is dominated by degree 5, a feature not found in other studies.

In a recent study, Dalton and Ekström (2006a, 2006b) considered a large global data set of Rayleigh-wave amplitudes in the period range 50–250 s. They inverted this data set, simultaneously, for maps of lateral variations in phase velocity up to spherical harmonics degree 20, attenuation, up to degree 12, as well as source and receiver correction factors. As in previous studies, the focusing effect is also included using expression [6]. A notable result of their study is the high quality phase velocity maps that they were able to obtain by using only the amplitude constraints in their inversion (Dalton and Ekström, 2006b). Inclusion of the source and receiver correction factors was also found to improve the attenuation mapping. They constructed maps of Rayleigh-wave attenuation at different periods, and also found a good correlation of the Q distribution with tectonics for periods sensitive to the first 250 km of the upper mantle (Dalton and Ekström, 2006a).

The studies described so far considered only fundamental mode surface waves which, in practice, limits the resolution in depth to the top 300–400 km of the upper mantle, even though some attempts at interpreting deeper structure were shown. These studies also used a two-step approach, and often only the results of the first step, inverting for maps of lateral variations of $q_R(\omega)$ at different periods, were presented (e.g., Romanowicz, 1990; Billien and Lévêque, 2000; Dalton and Ekström, 2006a). The more recent 3-D attenuation models include both even and odd terms of lateral heterogeneity in Q_μ (Romanowicz, 1995; Selby and Woodhouse, 2002), or in Q_R (Dalton and Ekström, 2006a). **Figure 6** compares maps of Q at a

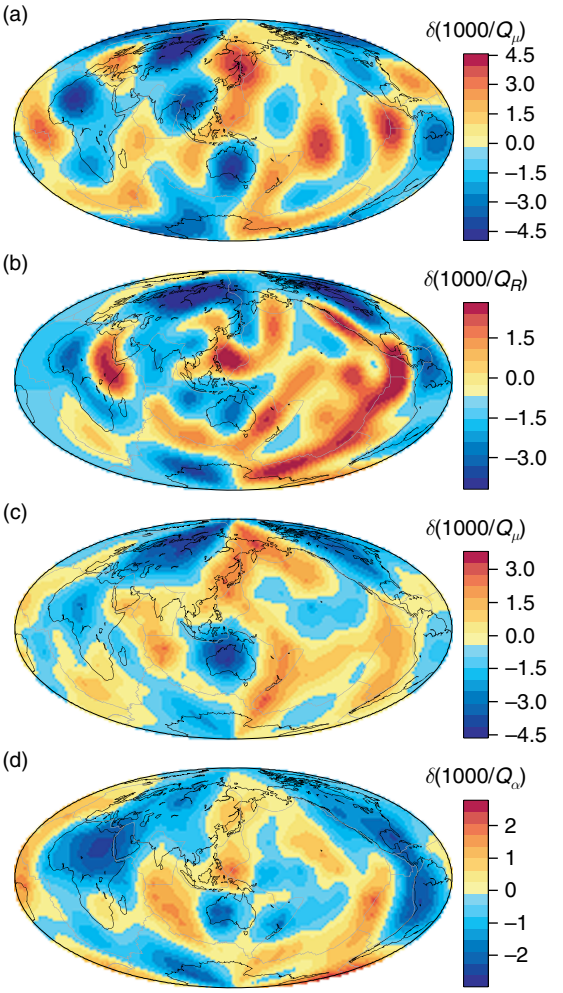

Figure 6 Comparison of global Q models in the uppermost mantle. (a) QRLW8 model (Gung and Romanowicz, 2004) from inversion of three component surface wave and overtone waveform data, presented is Q_μ at a depth of 160 km. (b) Map at 150 s of the Rayleigh wave Q model of Dalton and Ekström (2006a). (c) Average Q_μ in the depth range 0–250 km from Selby and Woodhouse (2002), also from Rayleigh waves. (d) Average variations in Q_α in the first 250 km of the mantle from amplitude ratios of P and PP (Warren and Shearer, 2002). Some of the differences observed may be due to the different depth ranges sampled: in models (a), (c), and (d), the global ridge and back-arc systems all stand out as low Q_μ features, whereas the Atlantic ridge is not as prominent in model (b), while the Red Sea region lights up more strongly. This may be due to the fact that (b) has not been inverted with depth, and therefore may include some effects of structure deeper than 250 km.

depth of 200 km obtained in different recent studies, and shows that, while details are still variable from model to model, the large scale features, with high Q in shield areas, low Q under ridges and back arcs, are quite consistent.

In order to improve the depth resolution in the transition zone, it is necessary to develop a methodology that includes information from surface-wave overtones, as well as Love waves. Because overtones are not easily separable due to their similar group velocities, a waveform methodology is desireable. Such a methodology uses a comparison of observed and synthetic seismograms in the time domain. The synthetics can be computed using normal mode theory, taking into account 3-D effects at various degrees of approximation. However, to obtain accurate amplitude information from surface-wave data, it is necessary to either employ an approach based on the measurement of envelopes, or to first align the timing of waveforms before comparing observed and synthetic waveforms. Following these considerations, Gung and Romanowicz (2004) recently developed an iterative waveform inversion approach, in which a large global data set of three-component fundamental and overtone waveforms, filtered in the frequency range 80–250 s, is first inverted for elastic 3-D structure, using the nonlinear asymptotic coupling theory (NACT) approach developed by Li and Romanowicz (1995), up to spherical harmonics degree 24. Different elastic models are computed for Love and Rayleigh waves, to account for the strong radially anisotropic signal in the uppermost mantle (e.g., Montagner and Tanimoto, 1991; Ekström and Dziewonski, 1997; Gung *et al.*, 2003). In a second step, the waveforms, corrected for the 3-D elastic structure obtained in the previous step, are inverted for lateral variations of $Q_\mu(r)$ in the upper mantle, up to degree 8. In this process the waveforms are directly inverted for depth dependence in elastic and anelastic structure.

Although Gung and Romanowicz (2004) did not include focusing effects in deriving their model QRLW8, subsequent tests indicated that the model was robust with respect to these effects, in agreement with the predictions of Selby and Woodhouse (2000). In particular, Gung and Romanowicz (2004) compared the degree 8 $Q_\mu(r)$ model obtained with and without focusing terms, the latter computed using expression [8] in the 3-D elastic model obtained in the first step, and found no significant changes. Including focusing in the second step of the inversion justifies inverting for a higher degree Q_μ model. **Figure 7** shows a comparison of the models obtained up to degree 12 and 16, in the transition zone, when focusing terms are included. Clearly, the large-scale features remain stable among the models, with some variability in the details. They indicate that, in contrast to the upper 200–300 km of the mantle, the main features in Q_μ in the transition zone are two large low Q regions in the south Central Pacific and under Africa, which correlate with the distribution of elastic velocities at the base of the mantle (Romanowicz and Gung, 2002), as well as the distribution of hotspots, confirming earlier results (Romanowicz, 1994b).

1.21.6.2 Global Body-Wave Studies

In the same way as differential traveltimes of teleseismic body-wave phases are used to obtain information on the distribution of upper mantle velocities, global scale lateral variations in attenuation can be inferred from differential amplitude measurements (i.e., amplitude ratios). These measurements are difficult, however, as they are sensitive to the window chosen for each phase, as well as to contamination by complex structure near the source, receiver, and bounce points. Komatitsch *et al.* (2002) have called attention to the importance of considering the effects of focusing and scattering in the crust. Chapter 1.05 provides details about the theoretical computation of the effects of attenuation on body waves.

Only three published studies to date have developed models of upper mantle Q based on differential body-wave measurements, two for Q_μ using S phases (Bhattacharyya *et al.*, 1996; Reid *et al.*, 2001) and one for Q_α (Warren and Shearer, 2002). Each of them used slightly different methods, but the basic principle remains the same.

The amplitude spectra of recorded body waves can be expressed as:

$$A(\omega) = cS(\omega)R(\omega)I(\omega)A_c(\omega)F\exp(-\omega t^*/2) \qquad [11]$$

where c is a constant expressing the radiation pattern and the geometrical spreading, $S(\omega)$ is the source spectrum, $R(\omega)$ the crustal response, $I(\omega)$ the instrument response, A_c is the crustal layering/reflectivity at the bounce point for reflected waves, and F is a hypothetical factor that includes possible effects of focusing. Also, t^* is defined as:

$$t^* = \int \frac{\mathrm{d}s}{Qv} \qquad [12]$$

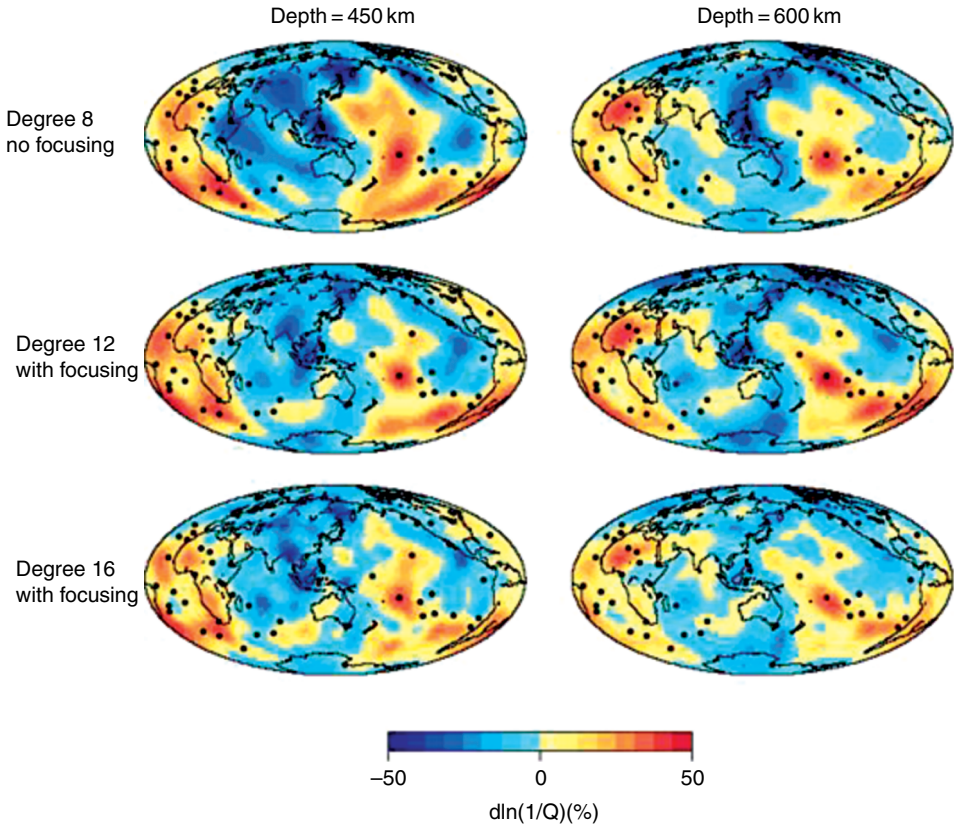

Figure 7 Lateral variations of Q_β in the upper mantle transition zone. (Top) Degree 8 Model QRLW8 (Gung and Romanowicz, 2004). In this relatively low degree model, no corrections for elastic focusing have been included. (Middle/bottom) Inversion of the same three component long period seismograms for a degree 12 model (middle) and a degree 16 model (bottom). In both cases, the waveforms have been corrected for focusing effects before inversion, using an asymptotic higher order formalism (Romanowicz, 1987). The main features of these models, namely strong low Q anomalies in the south Pacific and under Africa, correlated with the hot spot distribution of (Davies, 1990) (black dots) and high Q anomalies under the western Pacific, remain stable, but the low Q features sharpen up in the higher resolution models.

where v is the elastic velocity, Q the quality factor, which may depend on frequency, and the integral is taken along the ray path. In body-wave studies, the frequency dependence of Q needs to be taken into account, because the measurements are performed at higher frequency (typically 0.15–1 Hz for P-waves and 0.05–0.1 Hz for S-waves), closer to the high frequency cutoff in the Earth's absorption band. The frequency dependence of Q is often expressed in terms of an absorption band model (eqn [2]). However, Warren and Shearer (2002) estimated the effect of frequency dependence on the attenuation of P-waves around a period of 1 s, and concluded that neglecting it did not significantly bias their measurements of lateral variations in Q_α. On the other hand, Reid *et al.* (2001) suggested that the frequency dependence might be absorbed in the source terms.

Pairs of phases are selected so as to eliminate as many factors as possible from their spectral amplitude ratio. The differential δt^* can then be obtained by measuring the slope of the remaining spectral ratio as a function of frequency:

$$\ln(A_2/A_1) = -\omega/2(\delta t^*) + \epsilon \qquad [13]$$

where ϵ is a constant containing the effects of differential radiation pattern, geometrical spreading, and focusing for the two phases. The assumption of frequency independence of $\delta t^* = t_2^* - t_1^*$ needs to be verified even if dispersion corrections have been applied, and this is usually done by checking the linearity of the slope, as well as the constancy of the phase of the complex spectral ratio.

Because the lateral variations of Q in the lower mantle are thought to be much smaller than in the

upper mantle, the differential t^* thus obtained is attributed to lateral variations of structure in the upper mantle under the bounce point of the reflected phase. Given the steep approach of the reflected rays at the bounce point and the relatively sparse global sampling, these measurements provide information about the average upper mantle lateral variations in Q but have little depth resolution.

This general principle of slope measurement was used by Bhattacharyya *et al.* (1996) and Warren and Shearer (2002). However, these authors used different approaches to correct for potential receiver and source biases. Bhattacharyya *et al.* (1996) considered the spectra of S and SS from the same records, in the distance range 40–120°, and the period range 15–25 s, then estimated the differential t^* by applying a multiple-record stacking technique, grouping the records by bounce point location, and assuming that effects of source, receiver, and path, outside of the common upper mantle path of the SS waves with common bounce location, would average out in the stacks. The bounce point location area over which the stacking was performed were caps of 5° radius, larger than the estimated Fresnel zones of the corresponding reflected waves. These authors used a frequency domain multitaper technique to minimize the effects of finite source duration and near-source or near-receiver structure complexity. They found a correspondence between the cap-averaged t^* and tectonic provinces, with, as expected, lowest attenuation under platforms and shields and highest attenuation under young oceans. In a second step, they inverted for a depth dependent model of Q_μ in the upper mantle, expanded laterally up to degree 8 in spherical harmonics, and assuming three layers in depth (20–220 km, 220–400 km, 400–670 km). Resolution experiments indicated that the best resolved layer was the deepest one, and the two shallower ones could not be distinguished uniquely.

Warren and Shearer (2002), on the other hand, considered independent data sets of P waveforms, in the distance range 40–80°, and PP waveforms in the distance range 80–160°. Working in the frequency domain, they first determined source and receiver terms for the P data set, using an iterative stacking procedure over common sources and common receivers. Then they assumed that the same source and receiver terms could be applied to the PP phases, since the two phases have similar takeoff angles, path lengths, and turning depths, given the distance ranges considered. They thus corrected the PP amplitude spectra using the source and receiver terms determined from the *P* spectra and estimated the residual t^* attributed to the upper mantle beneath the bounce point. Finally, to reduce the scatter in the data, they estimated cap averages over nonoverlapping bounce point areas of 5° radius. They too found the highest Q_α (smallest t^*) under shields and platforms and the lowest Q_α (largest t^*) under young oceans. Unlike Bhattacharyya *et al.* (1996), these authors considered, however, that their measurements reflected the average structure over the top 220 km of the mantle and derived the corresponding Q_α averaged over that depth range.

Reid *et al.* (2001) developed a somewhat different method, based on waveform fitting, which they applied to a large data set of SS and S waveforms from seismograms collected in the distance range 50–105° and also to SSS, SS, in the distance range 90–179°. In the process, they included the effects of elastic structure on differential traveltimes of these phases. These authors considered that their data had sensitivity down to 400 km and inverted their t^* data set for a model of Q_μ expanded laterally to degree 8 and in depth, using a spline parametrization with six knots. However, their resolution tests indicated that the depth resolution was poor, and that they could not attribute the lateral variations found to a particular depth.

1.21.6.3 Multiple ScS Studies

Although they do not provide a complete global coverage, the most widely used shear-wave phases for large scale regional mantle attenuation studies have been multiple ScS phases. Measurements of the attenuation of these near-vertical multiply reflected waves are relatively uncontaminated by source, instrument, and geometrical spreading effects. They and their depth phases appear very clearly on transverse seismograms in the 'reverberative interval', after the first arriving surface-wave train (**Figure 8**). In the absence of noise, the transfer function relating ScS_n to ScS_{n+1} is, in the spectral domain:

$$H(\omega) = \exp[-\omega T_0/2Q(\omega)] \cdot \exp[i\theta(\omega, T_0)] \qquad [14]$$

where T_0 is the differential travel time between the two phases, θ is a phase function, and $Q(\omega)$ is the quality factor, which is an estimate of the vertically averaged attenuation through the mantle. As in the case of other differential measurements, the estimate of Q_{ScS} is obtained by measuring the slope of the amplitude of the transfer function as a function of frequency.

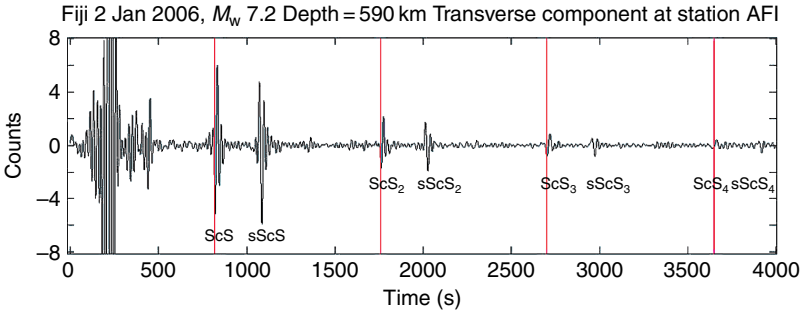

Figure 8 Example of multiple ScS record for a deep earthquake in the Fiji Islands, showing clear multiples out to ScS_4, as well as their depth phases. Courtesy of Ved Lekic.

The stability of the phase spectrum is used as an additional indication of the quality of the measurement.

Early studies used spectral ratios measured on hand-digitized and hand-rotated transverse component seismograms, and provided evidence for large amplitude lateral variations of Q_{ScS} in the mantle (e.g., Press, 1956; Kovach and Anderson, 1964; Sato and Espinosa, 1967; Yoshida and Tsujiura, 1975). Because of the analog records used, and the measurement methods employed, which did not take into consideration the biasing effects of noise, these early estimates are considered to be less accurate than more recent ones. They are also generally biased toward very high values of Q_{ScS}, compared to normal mode results, which has been a attributed not only to the effects of noise but also, potentially, to the effect of frequency dependence of Q, as the instruments which produced the records had limited bandwidth. With the advent of digital long period instrumentation, and the development of more sophisticated methods which were better suited for minimizing the effects of noise (e.g., Jordan and Sipkin, 1977; Nakanishi, 1979a), measurements became more accurate. For example, Jordan and Sipkin (1977) introduced a method of phase equalization, by computing cross-correlation between successive ScS multiples, as well as stacking to reduce measurement scatter. Nakanishi (1979a) used a maximum likelihood method to reduce the effects of noise. Most measurements are performed in the frequency band between 10 and 40–60 mHz, where frequency dependence of Q_{ScS} has been found to be negligible (e.g., Sipkin and Jordan, 1979). These studies have confirmed the existence of large lateral variations in Q_{ScS} (e.g., Sipkin and Jordan, 1980; Lay and Wallace, 1983, 1988; Chan and Der, 1988; Revenaugh and Jordan, 1989, 1991; Sipkin and Revenaugh, 1994; Suetsugu, 2001; Gomer and Okal, 2003). The derived average mantle values for $Q_\mu \sim 220$–240 are, in general, compatible with those obtained from normal modes.

Measurements under oceans, and in the vicinity of subduction zones are more numerous, because of the availability of deep earthquakes and the relatively simple effects of the thin crust at the surface reflection points. Measurements under continents are more difficult, because the effect of crustal multiples at the surface reflection point needs to be taken into account (e.g., Sipkin and Revenaugh, 1994; Isse and Nakanishi, 1997). In order to expand the coverage under continents, it is also necessary to consider shallow earthquakes, for which the reverberation interval is more noisy because of the presence of strong multipathing surface waves.

These studies determined that Q_{ScS} is higher under continents than under ocean basins, on average. Regional variability on relatively short scales has been found in subduction zone regions. In particular, low Q was estimated under the Sea of Japan (e.g., $Q_{ScS} \sim 160$, Nakanishi (1979a)) and under northern South America ($Q_{ScS} \sim 93$, Lay and Wallace (1983)), in regions sampling the upper mantle wedge and/or back-arc region behind subduction zones, which, if primarily attributed to the upper mantle, translates into very low Q. On the other hand, high Q values comparable to continental estimates were obtained on paths sampling through slabs (e.g., $Q_{ScS} \sim 232$, in South America, Lay and Wallace (1983); $Q_{ScS} \sim 226$, under Japan/Kuriles, Nakanishi (1979a); $Q_{ScS} \sim 266 \pm 57$ in Argentina, Sipkin and Jordan (1980)). These older measurements are generally in agreement with a more recent study by Chan and Der (1988), except in the southwest Pacific, where these authors found $Q_{ScS} \sim 214 \pm 42$ compared to the estimate of $Q_{ScS} \sim 157 \pm 17$ Sipkin and Jordan (1980). This may however be due to the way the latter averaged their measurements over an

extended region where strong lateral variations in Q_{ScS} have since been confirmed (Suetsugu, 2001; Gomer and Okal, 2003). Using short epicentral distance data (< 20°) filtered between 10 and 50 mHz, Suetsugu (2001) found very low Q under the south Pacific superswell ($Q_{ScS} \sim 70$–80) whereas Gomer and Okal (2003) found very high Q under the Ontong Java Plateau, also using short distances (10–20°) and a bandpass between 10 and 62.5 mHz.

The lateral variations found in Q_{ScS} are attributed primarily to the upper mantle, because of the much higher Q in the lower mantle, which reduces the effects on multiple ScS of any, even significant, lateral variations (e.g., Warren and Shearer, 2002), and the significant correlation of Q_{ScS} with tectonics. Furthermore, the correlation with travel time anomalies from the same multiple ScS phases suggests that they could be primarily related to lateral variations in temperature.

Caution must be exercised, of course, in attributing all of the Q_{ScS} signal to the upper mantle, in particular if there is a low Q zone at the base of the mantle (e.g., Revenaugh and Jordan, 1991), and significant lateral variations of Q in D″. While attenuation in D″ and its variations have yet to be explored at the global scale, the presence of large variations in velocity imply that at least some lateral variations exist in Q as well. Recently, Fisher and Wysession (2003) showed evidence for the existence of an ~600 km wide high-attenuation, low-velocity region in D″ beneath Central America, using spectral ratios of S and ScS phases.

1.21.6.4 Other Body-Wave Studies

High attenuation has been reported in the back of island arcs using other types of body waves. Early estimates were very qualitative (e.g., Barazangi and Isaaks, 1971; Barazangi *et al.*, 1975; Bowman, 1988). More recently, several regional studies (e.g., Flanagan and Wiens, 1990, 1994; Roth *et al.*, 1999, 2000) have utilized shear depth phases from deep earthquakes observed teleseismically or at regional arrays, to obtain constraints on the attenuation in the wedge of upper mantle above different subduction zones. Flanagan and Wiens (1990) measured differential attenuation between sS–S and sScS–ScS phase pairs beneath the Lau back-arc spreading center in the Fiji–Tonga region. Studying the variation of the estimated Q as a function of depth of the source, they found high attenuation in the first 200–300 km, and decreasing attenuation at greater depth. They found very high attenuation ($Q \sim 20$–35) in the uppermost mantle beneath the spreading center and somewhat lower attenuation ($Q \sim 50$) beneath older parts of the Lau Basin. Flanagan and Wiens (1994) extended this approach to the study of several inactive back-arc basins in the western Pacific, and confirmed the presence of high attenuation ($Q \sim 40$–50) in the uppermost mantle (depths less than 160 km), with even lower Q's (<40) in the vicinity of the volcanic centers. They also confirmed a systematic increase of Q with depth ($Q \sim 115$ between 160–430 km and $Q \sim 173$ in the transition zone). The frequency band of these two studies was 10–80 mHz.

Following the method of Teng (1968), Roth *et al.* (1999) assembled a data set of differential S–P and P–P attenuation measurements from a temporary local array of broadband land and ocean bottom stations in the Tonga–Fiji region. The data set they assembled allowed them higher resolution compared to teleseismic data because of the geometry of the source-station distribution, the short paths, and the small Fresnel zones compared to teleseismic phases. These authors measured δt from spectral ratios and obtained an estimate of the best fitting Q_α/Q_β ratio as part of the inversion for Q_α and Q_β, assuming that Q is not frequency dependent in the band-pass of their study (0.1–3.5 Hz), which seems to be verified by the data. They confirmed the high attenuation values in the uppermost mantle found previously beneath the spreading center. They then performed a 2-D tomographic inversion, assuming that the structure is uniform in the direction parallel to slab strike. In their model, the slab appears as a high Q zone ($Q_\alpha > 900$) down to at least 400 km, below which it is indistinguishable from the surrounding mantle. An abrupt transition from the high Q slab to the low Q back-arc basin occurs approximately at the Tonga volcanic front. The lowest Q_α values (~90) are found directly under the Lau back-arc spreading center. There is also evidence for a North–South trend, with attenuation on average higher by 10% in the northern part of the region. This Q tomographic model correlates well with velocity models in the region. The best fitting ratio Q_α/Q_β is ~ 1.75, which is in agreement with a loss in bulk about 1/3 that of the loss in shear, assuming a Poisson solid (**Figure 9**).

A similar study under the northern Philippine Sea, this time using only S–P spectral ratios (Shito and Shibutan, 2003b), found that the Philippine and Izu Bonin slabs also had high Q, and found low Q under the spreading center in the Shikoku Basin. However, the lowest values of Q were found at larger depths

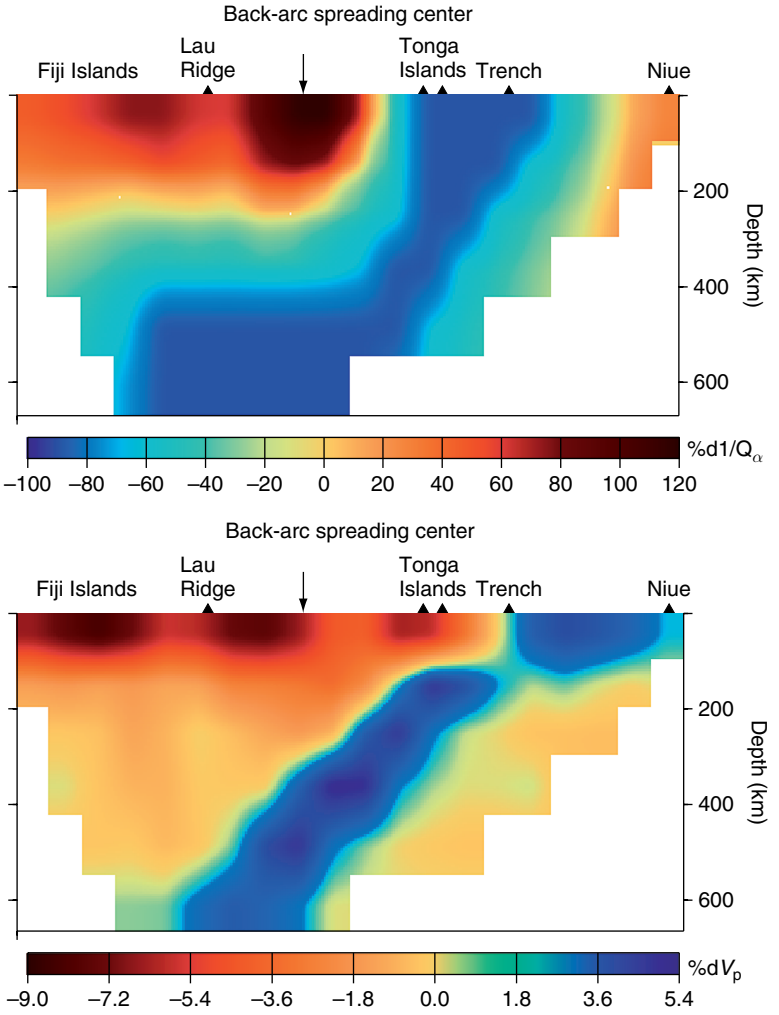

Figure 9 Cross section illustrating ateral variations of structure in the Lau back-arc basin. (Top) Attenuation, (bottom) velocity (V_p). Reproduced from Roth E, Wiens DA and Zhao D (2000) An empirical relationship between seismic attenuation and velocity anomalies in the upper mantle. *Geophysical Research Letters* 27: 601–604.

(250 km) than in the Lau Basin. The authors attributed that to the older age of the Shikoku spreading center.

Just as the upper mantle is found to be highly attenuating under back-arc spreading centers, other studies have investigated mid-ocean ridge systems and found very low Q (Molnar and Oliver, 1969; Solomon, 1973; Sheehan and Solomon, 1992; Ding and Grand, 1993). Sheehan and Solomon (1992) used the pair of teleseismic phases S and SS along the north-Atlantic ridge and found that SS-S differential attenuation decreases with increasing age of the oceanic plate, and that, in order for their measurements to be compatible with surface-wave studies, the high attenuation region must extend into the asthenosphere. Ding and Grand (1993) performed waveform modelling of multiple S phases (up to S_4) at distances between 30° and 80° along the East Pacific Rise. Because their data have sensitivity to the deep mantle, they found that, in order for their measurements to be compatible with multiple ScS results, a significantly lower average Q in the lower mantle is needed than obtained on average from normal mode measurements, indicating that lateral variations in Q may also exist in the lower mantle. Note that Sipkin and Jordan attributed a lower Q in the Fiji–KIP corridor from multiple ScS measurements to frequency dependence. In the light of the Ding and Grand (1993) study, it seems more likely that the observations of Sipkin and Jordan (1979) could just be due to lower Q's in the lower mantle, especially as both studies sampled regions of the Pacific Superplume.

In the last decade, there have been increasing efforts to interpret tomographic models of the upper mantle at various scales in terms of temperature, degrees of partial melt, water content, and rock composition, using constraints from elastic and anelastic tomography, heat flow, gravity, and experimental data. Thus, Sobolev *et al.* (1996) found that the Massif Central in France is underlain by a hot mantle body with a potential temperature 100–200°C higher than the upper mantle average. In an interpretation of velocity and Q tomography under the Philippine Sea, Shito and Shibutan (2003a) found that the deeper upper mantle (300–400 km depth) may contain 10–50 times more water than average. Boyd and Sheehan (2005) measured differential t^* of *S*-phase waveforms from the Rocky Mountain Front broadband network and found a north–south zone of very low Q_μ in the upper mantle beneath the Rocky Mountains. Combining attenuation and velocity data, they inferred that the Colorado Rocky Mountains are supported by low density mantle and a thick crust. On the other hand, comparing their laboratory measurements of Q_μ with global seismological Q models, Faul and Jackson (2005) inferred that the upper mantle low velocity zone could be explained by solid state processes, without invoking partial melting. Lawrence *et al.* (2006) applied a waveform cross-correlation method and cluster analysis to the study of upper mantle P and S-wave attenuation across the North American continent and found that the distribution of attenuation is in general correlated with that of velocity, implying higher temperatures beneath the western tectonic regions than under the more stable east, in agreement with both global and crustal continental scale studies.

In general t^* measurements, as well as surface-wave attenuation measurements are interpreted in terms of anelastic attenuation, however, contributions from scattering can be important and need to be considered. For example, in a study of S-wave amplitude variations under Iceland, (Allen *et al.*, 1999) found that the low velocity cylindrical-shaped plume acts as a lens, causing frequency dependent focusing that dominates over anelastic effects on the amplitudes.

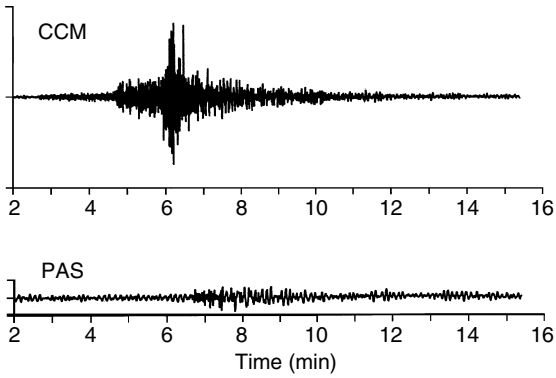

Figure 10 Seismograms recorded at stations CCM (Cathedral Cave, MO) and PAS (Pasadena, CA) for the m_b 4.5 event in southeastern New Mexico that occurred on 2 Jan 1992 at 11:45:35.6 UT. The epicentral distance to CCM (along a relatively high-Q path) is 1256 km and to PAS (along a relatively low-Q path) is 1417 km. From Mitchell BJ (1995) Anelastic structure and evolution of the continental crust and upper mantle from seismic surface wave attenuation. *Reviews of Geophysics* 33: 441–462.

1.21.7 Regional Q Variations in the Crust and Uppermost Mantle

1.21.7.1 Introduction

One of the most interesting aspects of Q in the crystalline crust and upper mantle of the Earth is the large magnitude of its variation from region to region. Whereas broad-scale seismic velocities vary laterally at those depths by at most 10–15%, Q can vary by an order of magnitude or more. **Figure 10** illustrates the large effect that regional Q variations can have on phases that travel through both the upper mantle (P and S waves) and the crust (Lg) by comparing records for paths across the eastern and western United States. Since variations in Q can be so large, seismic-wave attenuation is often able to relate Q variations to variations in geological and geophysical properties that are not easily detected by measurements of seismic velocities. Factors known to contribute to Q variations in the crust and upper mantle include temperature and interstitial fluids.

In this section we will emphasize studies of Q variation conducted over regions sufficiently broad to contribute to our knowledge of crust and upper mantle structure and evolution. In so doing we neglect many studies that have provided useful information on crustal Q over small regions.

1.21.7.2 *Q* or Attenuation Determinations for Seismic Waves in the Crust

Investigators have employed different methods, phases, and frequency ranges to study the anelastic properties of the crust and upper mantle. At higher frequencies and shorter distances often employed

for crustal studies some researchers have emphasized determinations of intrinsic Q (Q_i), some have emphasized the scattering contribution (Q_s), and some have sought to determine the relative contributions of Q_i and Q_s. The importance of scattering became apparent from the groundbreaking work of Aki (1969) who first showed that the codae of various regional phases are composed of scattered waves. His work spawned a large literature on both theoretical and observational aspects of scattering that is discussed in Chapter 1.20.

The contributions of the intrinsic and scattering components to total attenuation, $1/Q_t$, can be described by

$$\frac{1}{Q_t} = \frac{1}{Q_i} + \frac{1}{Q_s} \qquad [15]$$

where Q_i and Q_s refer, respectively, to intrinsic and scattering Q (Dainty, 1981). Richards and Menke (1983) verified that the contributions of intrinsic and scattering attenuation are approximately additive as described by eqn [15]. Seismologists often wish to focus on Earth's intrinsic anelastic structure. To do so they must select a phase or work in a frequency range such that the effect of scattering can either be determined or is small relative to the effect of intrinsic Q.

This review almost entirely addresses intrinsic Q, but we will discuss one type of scattered wave (Lg coda) quite extensively. Although Lg coda is considered to contain a large amount of scattered energy, some theoretical and computational studies (discussed later) of scattered S-wave energy suggest that measured Q values for that wave may largely reflect intrinsic properties of the crust.

All of the measurements that we discuss in this section can be placed in one of two major categories: (1) those in which seismic source effects cancel and (2) those in which assumptions are made about the seismic source spectrum. For category (1) the cancellation is most often achieved by using ratios of amplitudes recorded by two or more instruments. But it has also been achieved using ratios of amplitudes from different portions of a single time series. The primary application of the latter type of cancellation has been for the determination of Lg coda Q (Q_{Lg}^{C}). We divide this category into three parts that address regional phases, fundamental-mode surface waves, and Lg coda. Category (2) permits studies of Q using a single station, but requires knowledge of the source depth, source mechanism, and velocity model for the source region. We divide this category into two parts, one addressing regional phases and the other fundamental-mode surface waves.

Seismologists have measured the dispersion of body waves due to anelasticity and have successfully used that dispersion to infer values for body-wave Q. We will not cover that topic because it has been the subject of relatively few studies and has been applied mainly to small regions.

The following subsections discuss methodology and present some representative results using the cited methods as applied to the crust. Because the number of studies for continents is overwhelmingly greater than for oceans, most of the discussion will pertain to continental regions. A few studies will, however, be described for oceanic regions.

1.21.7.2.1 Spectral decay methods in which source effects cancel – Regional phases

Regional phases include P, S, and Lg phases recorded at distances less than about 1000 km. The early portion of this section mostly covers Q determinations for P and S phases but in cases where researchers measured Q_{Lg}, as well as Q_P and Q_S all results will be presented. The latter part of this subsection will discuss Lg exclusively since this phase has been widely used in recent years to study variations of Q over broad regions.

In order to cancel the source effects, several methods utilize stations that lie on a common great-circle path with the seismic source but other methods are able to dispense with the need for great-circle path propagation. All studies, however, need to first remove the effect of wave-front spreading before measuring amplitude changes due to attenuation. In this subsection we will restrict our discussion to studies at frequencies that pertain totally or predominantly to the crust with occasional reference to the upper mantle for studies that include results for both the crust and upper mantle.

Regional and near-distance studies of P- and S-wave attenuation (or their respective quality factors Q_P and Q_S) often cancel the source by utilizing several stations at varying distances (e.g., Nuttli, 1978, 1980; Thouvenot, 1983; Carpenter and Sanford, 1985)

More recently, amplitude measurements in which both the source and sensor reside in boreholes beneath any sediments or weathered layers have provided much-improved estimates of Q_P and Q_S. Abercrombie (1997) used borehole recordings to determine spectral ratios of direct P- to S-waves

and found that they are well modeled with a frequency-independent Q_P distribution in the borehole increasing from $Q_P \sim 26$–133 at depths between the upper 300 m and 1.5–3 km. Q_S increased from 15 to 47 in the same depth range. Abercrombie (2000), in another borehole study near the San Andreas Fault, found that attenuation on the northeastern side of the fault is about twice that on the southwestern side.

Lg is very useful for Q studies both because it travels predominantly in the crustal waveguide, providing Q information for a known depth interval, and is a large and easily recognizable phase. Even relatively small earthquakes can generate useable records; thus data, in many regions is plentiful. Lg can be represented by a superposition of many higher-mode surface waves or by a composite of rays multiply reflected in the crust. It is usually assumed that Q_{Lg} follows a power-law frequency dependence, $Q = Q_o f^{\eta}$, where Q_o is the value of Q_{Lg} at a reference frequency and η is the frequency dependence parameter at that frequency. Lg travels through continental crust at velocities between about 3.2 and 3.6 km s^{-1} and is usually followed by a coda of variable duration. That coda is discussed in a later subsection. Since the Lg wave consists of many higher modes, it is often assumed that, even though the radiation patterns for individual modes differ from one another, the totality of modes combine to form a source radiation pattern that is approximately circular. If that assumption is correct the source and stations need not necessarily line up along the same great-circle path to estimate Q.

Early determinations of Q_{Lg}, after correcting for wave-front spreading, compared observed attenuation with distance with theoretically predicted attenuation for the Lg phase and chose the theoretical curve (predicted by selected values of Q_o and η) which agreed best with observations (e.g., Nuttli, 1973; Street, 1976; Bollinger, 1979; Hasegawa, 1985; Campillo *et al.*, 1985; Chavez and Priestley, 1986; Chun *et al.*, 1987).

Benz *et al.* (1997) studied four regions (southern California, the Basin and Range province, the central United States, and the northeastern United States and southeastern Canada) of North America in the frequency range 0.5–14.0 Hz. They found that, at 1 Hz, Q_{Lg} varies from about 187 in southern California to 1052 in the northeastern United States and southeastern Canada and about 1291 in the central United States. They also found that the frequency dependence of Q also varies regionally, being relatively high ($\alpha \sim 0.55$–0.56) in southern California and the Basin and Range and smaller ($\alpha \sim 0$–0.22) in the other three regions.

Xie and Mitchell (1990a) applied a stacking method to many two-station measurements of Q_{Lg} at 1 Hz frequency in the Basin and Range province. This method, first developed for single-station determinations of Lg coda Q (Q_{Lg}^{C}), will be discussed in the subsection on Lg coda. They found that $Q_{Lg} = (275 \pm 50) f^{(0.5 \pm 0.2)}$ and $Q_{Lg}^{C} = (268 \pm 50) f^{(0.5 \pm 0.2)}$.

Xie *et al.* (2004) extended the method to multiple pairs of stations in instrument arrays across the Tibetan Plateau. For an array in central Tibet (INDEPTH III) they found very low values for Q_o ($\sim$90) that they attributed to very high temperatures and partial melt the crust. An array in southern Tibet yielded even lower values, $\sim$60, for Q_o in the northern portion of the array but higher values ($\sim$100) in a central portion and much higher values (>300) in the southernmost portion. Xie *et al.* (2006) used a two-station method to obtain more than 5000 spectral ratios for 594 interstation paths and obtained Q_o and η for those paths. They obtained tomographic maps of those values that are described in the subsection on tomographic mapping.

1.21.7.2.2 Spectral decay methods in which source effects cancel – Fundamental-mode surface waves

When using fundamental-mode surface waves to study lateral variations of crustal Q_μ we need to measure the attenuation of relatively short-period (5–100 s) amplitudes. In continents, these waves may be biased by systematic errors associated with laterally varying elastic properties along the path of travel, as discussed earlier. Two-station studies of fundamental-mode surface waves are especially susceptible to these types of error because researchers might incorrectly assume great-circle propagation along a path through the source and the two stations. Non-great-circle propagation would mean that surface-wave energy arriving at two stations along different great-circle paths could originate at different portions of the source radiation pattern. If that pattern is not circular the two-station method can produce attenuation coefficient values that are either too high or too low, depending on the points of the radiation pattern at which the waves originate.

Measurements for the situation in which a source and two stations lie approximately on the same great-circle path have often been used to determine surface-wave attenuation. The method was described by Tsai and Aki (1969) and determines the average

surface-wave Q between the two stations after correcting for the different wave front spreading factors at the two stations. They applied the method to many two-station paths from the Parkfield, California earthquake of 28 Jun 1966 and, using the formulation of Anderson *et al.* (1965), obtained a frequency-independent model of intrinsic shear-wave Q (Q_μ) with a low-Q zone that coincided with the Gutenberg low-velocity zone in the upper mantle. Love-wave Q was greater than 800 and Rayleigh-wave Q was greater than 1000 in the period range 20–25 s.

Other studies using that method to obtain Q_μ models at crustal and uppermost mantle depths include Hwang and Mitchell (1987) for several stable and tectonically active regions of the world, Al-Khatib and Mitchell (1991) for the western United States and Cong and Mitchell (1998) for the Middle East.

Models have also been obtained in which Q_μ varies with frequency. That frequency dependence is described by the relation $Q_\mu = Q_o f^\zeta$ where ζ may vary with frequency (Mitchell, 1975) and/or with depth (Mitchell and Xie, 1994). The inversion process for Q_μ in those cases requires appropriate extensions of the Anderson *et al.* (1965) equations. The process requires both fundamental-mode surface-wave attenuation data and Q or attenuation information for either an individual higher mode or the combination of higher modes that form the Lg phase. The process proceeds by assuming a simple one- or two-layer distribution of ζ and inverting the fundamental-mode data for a Q_μ model. ζ is adjusted until a Q_μ model is obtained that explains both the fundamental-mode and higher-mode attenuation data. Mitchell and Xie (1994) applied the method to the Basin and Range province of the western United States. Example Q_μ models for which ζ varies with depth (Mitchell and Xie, 1994) appear in **Figure 11**.

Other surface-wave studies for which the source is cancelled are those that use many stations at various distances and azimuths and simultaneously solve for surface-wave attenuation coefficient values and seismic moments for particular periods by linear least squares. Tryggvason (1965) first did this, as described in our section on early studies, using explosions and assuming circular radiation patterns. Tsai and Aki (1969) extended this method to use earthquake sources, and applied it to surface waves generated by the 28 Jun 1966 Parkfield, California earthquake. This process was later applied to the central United States (Mitchell, 1973; Herrmann and Mitchell, 1975), and the Basin and Range province of the western United States (Patton and Taylor, 1989).

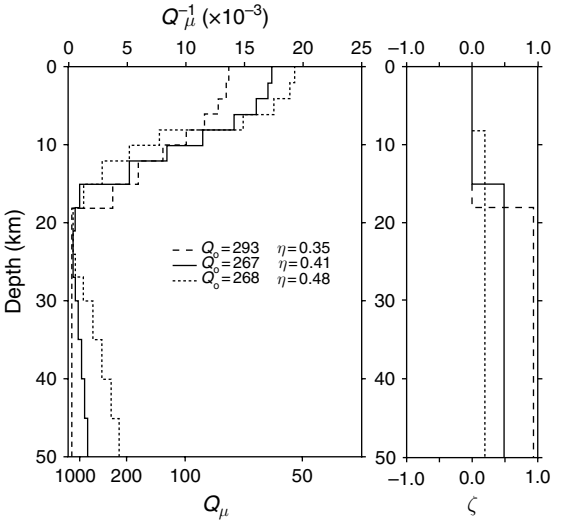

Figure 11 (Left) Three Q_μ models resulting from inversion of Rayleigh-wave attenuation coefficient data from the Basin and Range Province. The numbers refer to the value of Q_o and η predicted by three models for Q_{LG}. (Right) Three selected models for the variation of Q_μ frequency dependence with depth in the crust of the Basin and Range province. Each of these depth distributions was fixed during inversions that produced Q_μ models. Reproduced from Mitchell BJ and Xie J (1994) Attenuation of multiphase surface waves in the Basin and Range province. Part III: Inversion for crustal anelasticity. *Geophysical Journal International* 116: 468–484, with permission from Blackwell Publishing.

A nonlinear variation of the Tsai and Aki method (Mitchell, 1975), represents a nuclear explosion with strain release by a superposition of an explosion (with a circular radiation pattern) and a vertical strike-slip fault (represented by a horizntal double couple). Variations of the orientation of the double couple and its strength relative to the explosion produce a wide variety of radiation patterns. The inversion solves for the moment of the explosion, the orientation of the double couple, the strength of the double couple relative to the explosion and an average attenuation coefficient value for each period of interest. Mitchell applied the method to two nuclear events in Colorado as recorded by stations throughout the United States and found that Q_μ in the upper crust of the eastern United States is about twice as high as it is in the western United States at surface-wave frequencies.

The first attempts at mapping regional variations of attenuation or Q utilized crude regionalizations (two or three regions) based upon broad-scale geological or geophysical information. Studies have produced

models for Eurasia (Yacoub and Mitchell, 1977) using the method of Mitchell (1975), and for the Pacific (Canas and Mitchell, 1978) and Atlantic (Canas and Mitchell, 1981) using the two-station method.

1.21.7.2.3 Spectral decay methods in which source effects cancel – Lg coda

Lg coda, like direct Lg, is sensitive to properties through a known depth range (the crust) in which it travels and is a large amplitude phase for which data are plentiful. In addition, since the coda of Lg is comprised of scattered energy, it can continue to oscillate for several hundred seconds following the onset of the direct Lg phase, thus making it possible to stack spectral amplitudes for many pairs of time windows to make a Q estimate. Other positive aspects of using Lg coda for Q studies are that the averaging effect of scattering stabilizes Q_{Lg}^{C} determinations and, if stacking methods are utilized to determine Q for Lg coda, site effects cancel (Xie and Mitchell, 1990a).

Two methods have been applied to Lg coda to make Q determinations. The first of these was developed by Herrmann (1980) and applied by Singh and Herrmann (1983) to data in the United States. The method extended the coda theory of Aki (1969) utilizing the idea that coda dispersion is due to the combined effects of the instrument response and the Q filter of the Earth. The two studies provided new approximations for the relative variation of Q across the United States. Herrmann later realized, however, that his method did not take into consideration the broadband nature of the recorded signal and overestimates Q by about 30% (R. B. Herrmann, personal communication).

Xie and Nuttli (1988) introduced the stacked spectral ratio (SSR) method which stacks spectra from several pairs of windows along the coda of Lg. That process leads to

$$R_k = f^{1-\eta}/Q_o \qquad [16]$$

as the expression for the SSR, or in logarithmic form

$$\log R_k = (1-\eta)\log f_k - \log Q_o + e \qquad [17]$$

from which Q_o and η can be obtained by linear regression. f_k, Q_o, η, and e in these equations are, respectively, a discrete frequency, the value of Q at 1 Hz, the frequency dependence of Q at frequencies near 1 Hz, and an estimate for random error. This stacking process provides stable estimates of Q_o and η with standard errors sufficiently low to allow tomographic mapping of those quantities. A detailed description of the SSR method appears in Xie and Nuttli (1988) and more briefly in Mitchell *et al.* (1997)

Figure 12 shows an example of Lg coda and its associated SSR for a relatively high-Q path in India, which can be fit over a broad frequency range with a straight line on a log–log plot. The value at 1 Hz provides an estimate of $1/Q$ at that frequency and the slope of the line gives an estimate for η. Inversions of sets of those values over a broad region can yield tomographic maps of those quantities.

Past studies have shown that several factors may contribute to reductions in Q_o; these include thick accumulations of young sediments (Mitchell and Hwang, 1987) and the presence of a velocity gradient rather than a sharp interface at the core–mantle boundary (Bowman and Kennett, 1991; Mitchell *et al.*, 1998). In addition, decreasing depth of the Moho in the direction of Lg travel or undulations of the Moho surface can be expected to decrease measured Q_{Lg} or Q_{Lg}^{C} whereas increasing depth would produce larger values. To our knowledge this effect has not been quantitatively studied and is expected to be small over large regions. These factors may cause determinations of correlation coefficients between Q_{Lg} or Q_{Lg}^{C} and various crustal or mantle properties to be relatively low whenever they are determined (e.g., Zhang and Lay, 1994; Artemieva *et al.*, 2004).

1.21.7.2.4 Spectral decay methods for which assumptions are made about the source spectrum – Regional phases

Hough *et al.* (1988) studied S-waves traveling over relatively short distances near Anza, California, and defined the instrument-corrected acceleration spectrum at a station located a distance r from the source as

$$A(r, f) = A_o e^{-\pi t^* f} \qquad [18]$$

where t^* is defined in eqn [12]. For crustal studies it is common to assume that Q is constant along the path, in which case

$$t^* = \frac{t}{Q} \qquad [19]$$

where t is the travel time.

Hough *et al.* (1988) defined A_o as

$$A_o = (2\pi f)^2 S(f) G(r, f) \qquad [20]$$

where $S(f)$ is the source displacement spectrum and $G(r, f)$ is the geometrical spreading factor which, if

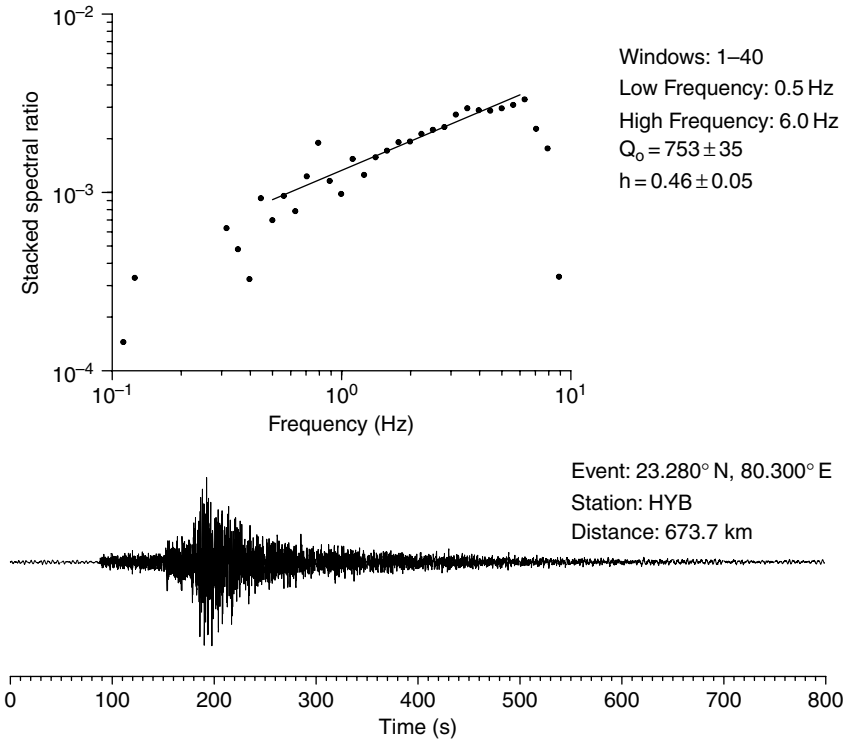

Figure 12 (Bottom) Seismogram, (Top) stacked spectral ratio (SSR) as a function of frequency for a relatively high-Q path in India.

we assume frequency-independent propagation in a homogeneous medium, is $1/r$ for body waves. At higher frequencies, these methods assume a spectral falloff rate (such as ω^{-2} or ω^{-3}) and attribute additional falloff to attenuation. Since a large body of data supports the ω^{-2}, or Brune, model (Brune, 1970) that is the one most commonly used. Taking the natural logarithm of eqn [18] leaves

$$\ln A(f) = \ln A_0 - \pi f t^* \qquad [21]$$

For the frequency-independent case, this equation defines a straight line with an intercept of $\ln A_o$ and a slope of $-\pi t/\underline{Q}_o$. Anderson and Hough (1984) hypothesized that, to first order, the shape of the acceleration spectrum at high frequencies can be described by

$$\alpha(f) = A_o e^{-\pi\kappa f} f > f_E \qquad [22]$$

where f_E is the frequency above which the spectral shape is indistinguishable from spectral decay and A_o depends on source properties and epicentral distance. They found that κ increased slowly with distance, an observation consistent with a $\underline{Q}$ model of the crust that increases with depth in its shallow layers and that it was systematically smaller on rock sites than at alluvial sites. Hough *et al.* (1988) studied κ as a function of hypocentral distance, as well as site and source characteristics, and found that $\kappa(0)$ differed for sites at Anza and the Imperial Valley in California but that $d\kappa/dr$ was similar for the two regions. Their interpretation was that $\kappa(0)$ was a component of attenuation that reflects $\underline{Q}_i$ in the shallow portion of the crust while $d\kappa/dr$ was due to regional structure at great depth. This method was applied to various regions in the world including the Canadian Shield (Hasegawa, 1974), the Pyrenees (Modiano and Hatzfeld, 1982), the New Madrid zone of the central United States (Al-Shukri *et al.*, 1988), and eastern Asia (Phillips *et al.*, 2000).

Shi *et al.* (1996) studied $\underline{Q}_{Lg}$ variation for five tectonically different regions of the northeastern United States. They used eight pairs of co-located earthquakes to determine accurate source spectrum corner frequencies by applying an empirical Green's function method to Pg and Lg or Sg phases. Based upon the corner frequencies, Sg or Lg displacement spectra were used to obtain values of $\underline{Q}$ and η values for 87 event-station paths at frequencies between 1 and 30 Hz. The 1 Hz $\underline{Q}_o$ values for the five regions vary between 561 and 905 while η varies between 0.40 and 0.47.

1.21.7.2.5 Spectral decay methods for which assumptions are made about the source spectrum – Fundamental-mode surface waves

A multimode spectral method has yielded simple crustal models (two or three layers) of shear-wave Q (Q_μ) in a few regions. The method assumes a flat source spectrum and tries to match theoretical amplitude spectra to two sets of observed spectral amplitude data, one corresponding to the fundamental mode and the other to the superposition of higher modes that forms the longer-period (3–10 s) component of the Lg phase. The higher modes travel faster than all but the longest-period fundamental-mode energy observed on records for relatively small events that are used with this method.

The first study using this method (Cheng and Mitchell, 1981) compared upper crustal Q_μ for three regions of North America and found values of 275 for the eastern United States, 160 for the Colorado Plateau, and 85 for the Basin and Range province. Kijko and Mitchell (1983) applied the method to the Barents Shelf, a region of relatively high-Q crystalline crust overlain by low-Q sediments. They found the method to be sensitive to Q_μ in the sediments and upper crust but insensitive to Q_μ in the lower crust and to P-wave Q at all depths. Cong and Mitchell (1998) obtained models in which Q_μ is very low at all depths beneath the Iran/Turkish Plateaus and somewhat higher, but still much lower than expected beneath the Arabian Peninsula. Models they obtained using the multimode method, agree well with those they obtained using the two-station method.

Jemberie and Mitchell (2004) applied the method to China and peripheral regions and obtained three-layer crustal models with low Q_μ and wide variation across China. Values decrease with depth beneath regions such as southeastern China and increase with depth beneath other regions such as the eastern Tibetan Plateau.

1.21.7.3 Tomographic Mapping of Crustal Q

Seismologists are currently attempting to map variations of Q and its frequency variation in the Earth in as much detail as possible. For continents, researchers have obtained tomographic maps for several broad regions using Lg coda, the direct Lg phase and surface waves. Studies using P and S-waves have yielded important results in regions where earth quakes and recording stations are plentiful. Studies of even smaller regions, such as volcanoes and geothermal areas, have utilized P- and S-waves (e.g., Hough *et al.*, 1999). In this review, we will restrict our discussion to the more broad-scale studies.

An earlier section described three early regionalized studies of surface-wave attenuation in the late 1970s and early 1980s, one for continental paths and two for oceanic paths in which the Eurasian continent, the Pacific Ocean, and Atlantic Ocean were divided into two or three regions. Since then tomographic mapping using Lg coda has made possible a much finer regionalization of crustal Q in continents. This section will discuss tomography results for continents and for one oceanic region using either direct Lg, fundamental-mode surface waves, P- and S-waves.

We emphasize Lg coda since tomographic maps of $Q_{\mathrm{Lg}}^{\mathrm{C}}$, all obtained for the same frequency, and using the same methodology, are available for all continents except Antartica. This commonality in phase, frequency, and method allows us to compare Q from one continent to that in others and also to various geophysical and geological properties. These comparisons contribute to our understanding of the mechanisms for seismic-wave attenuation in the crust.

Earlier sections have indicated that Lg coda has several properties that make it useful for tomographic studies. First, it is usually a large amplitude phase making it easily available for study in most regions of the world. Second, it is a scattered wave and the averaging effect of that scattering makes Lg coda relatively insensitive to focusing. Third, the SSR method used to determine Q_{o} and η tends to cancel site effects. Fourth, although it is a scattered wave, measurements of Q for seismic coda have been shown theoretically and computationally to yield measures of intrinsic Q (e.g., Frankel and Wennerberg, 1987; Mitchell, 1995; Sarker and Abers, 1999). If that is correct researchers can interpret Q variation in terms of Earth structure and evolution. Other studes, however, (e.g., Aki, 1980; Gusev and Abubakirov, 1996) attribute energy loss to scattering. The mechanism, at this point must therefore be considered controversial.

As indicated earlier, Lg coda Q ($Q_{\mathrm{Lg}}^{\mathrm{C}}$) is typically assumed to follow a power-law frequency dependence, $Q_{\mathrm{Lg}}^{\mathrm{C}} = Q_{\mathrm{o}} f^{\eta}$, where Q_{o} is the Q value at 1 Hz and η is the frequency dependence of Q near 1 Hz. Tomographic maps of the 1 Hz values of $Q_{\mathrm{Lg}}^{\mathrm{C}}$ (Q_{o} and η) with nearly continent-wide coverage are now

available for Eurasia (Mitchell *et al.*, 1997, 2007), Africa (Xie and Mitchell, 1990b), South America (DeSouza and Mitchell, 1998), and Australia (Mitchell *et al.*, 1998). In North America, broad-scale determinations of Q_{Lg}^{C} are currently restricted to the United States (Baqer and Mitchell, 1998). These studies have shown a wide range of average Q_o values for different continents and a very wide range within each continent. Average Q_o tend to be highest in continents that contain the most old stable cratonic regions that have not undergone later tectonic or orogenic activity (e.g., Africa and South America).

Tomographic studies have also been completed for more restricted regions using the direct Lg phase in Eurasia, North America, and South America and high-resolution tomographic maps of Q for P- and S-waves are available for southern California. For oceanic regions, tomographic mapping of Q variations, to our knowledge, is currently available only for P waves in one broad portion of the East Pacific Rise (Wilcock *et al.*, 1995).

Sarker and Abers (1998) showed that, for comparative studies, it is important that researchers use the same phase and methodology in comparative Q studies. The Lg coda Q maps presented here adhere to that principle; thus the continental-scale maps of Q_o and η for Lg coda at 1 Hz that are available can be considered to provide the closest thing to global Q coverage at crustal depth that currently exists. The maps also present the possibility for comparisons of Q_o variation patterns with variations of seismic velocity, temperature, plate subduction, seismicity, the surface velocity field, and tectonics when that information is available.

A discussion of the inversion method for mapping Q_o and η appears, in detail, in Xie and Mitchell (1990b), and more briefly, in Mitchell *et al.* (1997). The method assumes that the area occupied by the scattered energy of recorded Lg coda can be approximated by an ellipse with the source at one focus and the recording station at the other, as was shown theoretically by Malin (1978) to be the case for single scattering.

Xie and Mitchell (1990b) utilized a back-projection algorithm (Humphreys and Clayton, 1988) to develop a methodology for deriving tomographic images of Q_o and η over broad regions using a number of Q_o or η values determined from observed ground motion. **Figures 13(a)**, **14(a)**, **15(a)**, **16(a)**, and **17(a)** show the ellipses that approximate data coverage for the event-station pairs used in Q_{Lg}^{C} studies of Eurasia, Africa, South America, Australia, and the United States. The inversion process assumes that each ellipse approximates the spatial coverage of scattered energy comprising late Lg coda. The areas of the ellipses grow larger with increasing lag time of the Lg coda components. The ellipses in the figure are plotted for maximum lag times used in the determination of Q_o and η. Ideally, each inversion should utilize many ellipses that are oriented in various directions and exhibit considerable overlap in order to obtain the redundancy needed to obtain the best possible resolution for features of interest. Xie and Mitchell (1990b) discuss the procedure in detail, presenting methods for obtaining standard errors for Q_o and η and for estimating spatial resolution.

Because Lg coda consists of scattered energy, it must be distributed, for each event-station pair, over an area surrounding the great-circle path between the source and receiver. Because of this areal coverage, our maps may not include effects of Lg blockage in regions where such blockage has been reported. We may have no data from blocked paths, but are likely to have other paths, such as those subparallel to the blocking feature or for which the source or recording station, represented by one focus of the scattering ellipse, lies near the blocking feature. In both cases portions of the scattering ellipses may overlap the blocking feature, but that feature will not substantially contribute to the values we obtain for Q_o and η. A comparison of mapped Q_o for all continents (Figures **13(b)**, **14(b)**, **15(b)**, **16(b)** and **17(b)**) shows that it is typically highest in the stable portions of continents and lowest in regions that are, or recently have been, tectonically active. Exceptions occur, however, especially for stable regions. For instance, the Arabian Peninsula, although being a stable platform shows Q_o variations between 300 and 450, values that are one-half or less of maximum values in other Eurasian platforms. Other regions showing lower than expected Q_o include the Siberian trap region of northern Siberia and the cratonic regions of Australia.

The frequency dependence values of Q_{Lg}^{C} (η) in Figures **13(c)**, **14(c)**, **15(c)**, **16(c)**, and **17(c)** appear to show consistent relationships to Q_o in some individual continents. For instance, in both Africa and South America, high-Q regions are typically regions of low η. That same relationship, however, does not occur consistently in Eurasia, Australia, or the United States. η is high, for instance, throughout much of the northern portions of Eurasia where Q_o is mostly high but is low in California, Kamchatka, and a portion of southeast Asia where Q_o is very low.

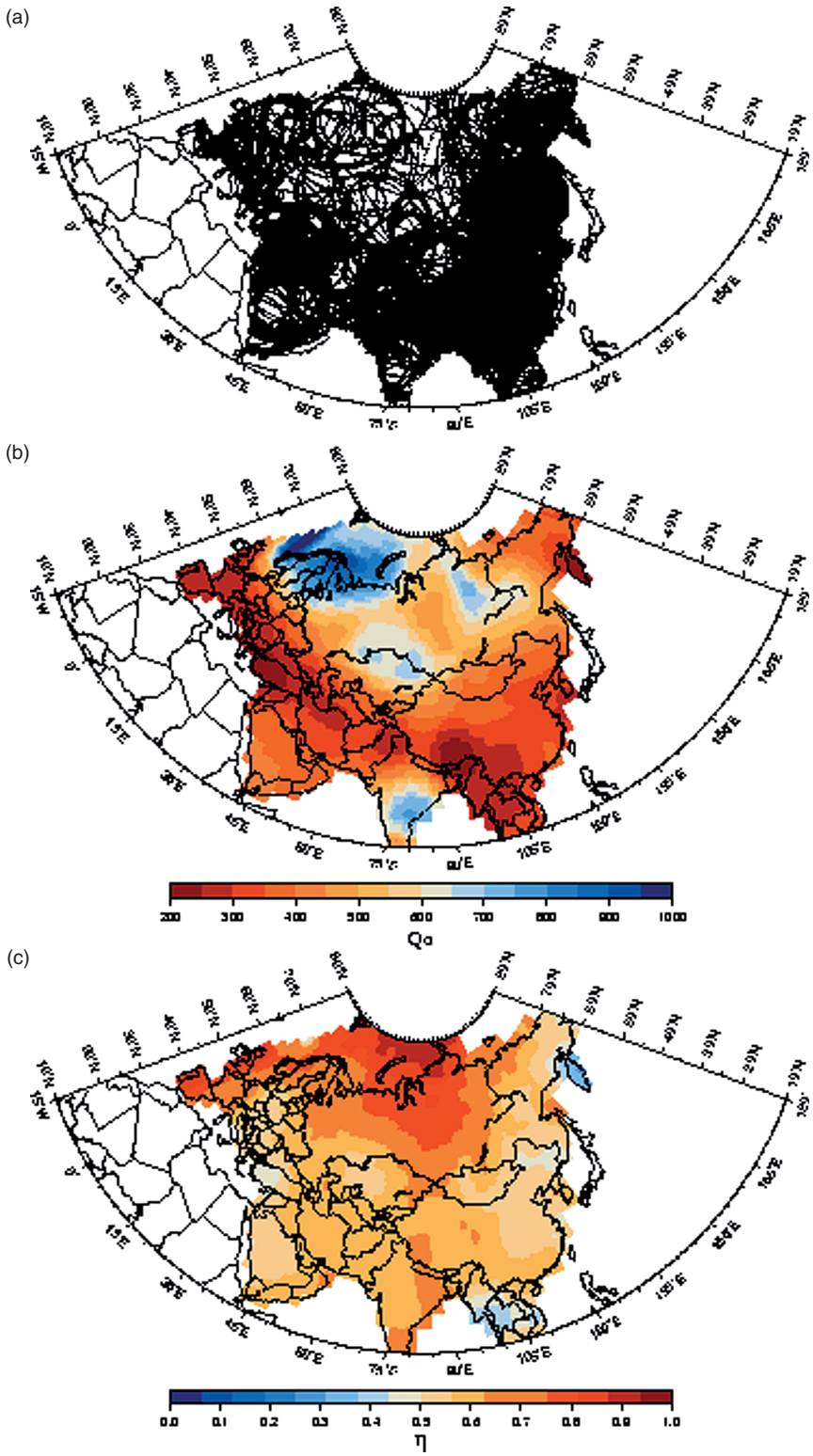

Figure 13 (a) A scattering ellipse map, (b) a Q_o map, and (c) an η map for Eurasia. Adapted from Mitchell BJ, Cong L, and Ekström G (2007) A continent-wide 1-Hz map of *Lg* coda *Q* variation across Eurasia and its implications for lithospheric evolution. *Journal of Geophysical Research* (in review).

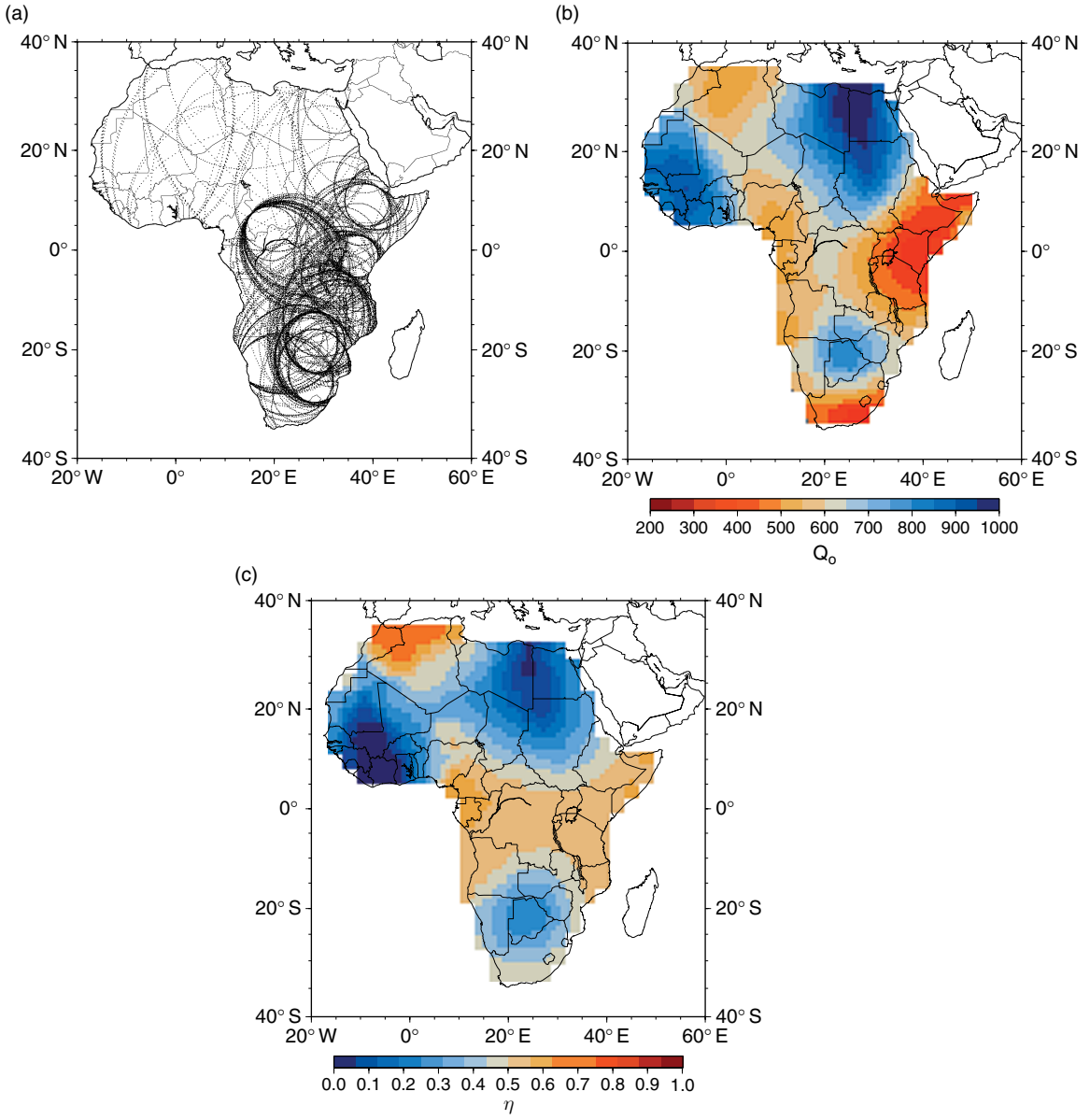

Figure 14 (a) A scattering ellipse map, (b) a Q_o map, and (c) an η map for Africa. Adapted from Xie J and Mitchell BJ (1990b) A back-projection method for imaging large-scale lateral variations of *Lg* coda *Q* with application to continental Africa. *Geophysical Journal International*100: 161–181.

1.21.7.3.1 Q^{C}_{Lg}, Q_{Lg}, and Q_{μ} tomography in regions of Eurasia

Figure 13 shows maps of data coverage, Q_o, and η across most of Eurasia (Mitchell *et al.*, 2007). These maps represent a major increase in data coverage for northeastern Siberia, southeastern Asia, India, and Spain, compared to those of an earlier study (Mitchell *et al.*, 1997) and provide additional redundancy in regions where there was earlier coverage. As indicated by **Figure 13(a)**, the data coverage is excellent for virtually all of Eurasia. Low Q_o values extend through the Tethysides belt that extends across southern Eurasia from western Europe to eastern China and its southern portions appear to be related to subduction processes occurring at the present time. Q_o is generally high in the platforms of northern Eurasia and India (600–950). It is, however, low in the Kamchatka Peninsula and regions directly north of there which, like the Tethysides region, are seismically active. A conspicuous region of relatively

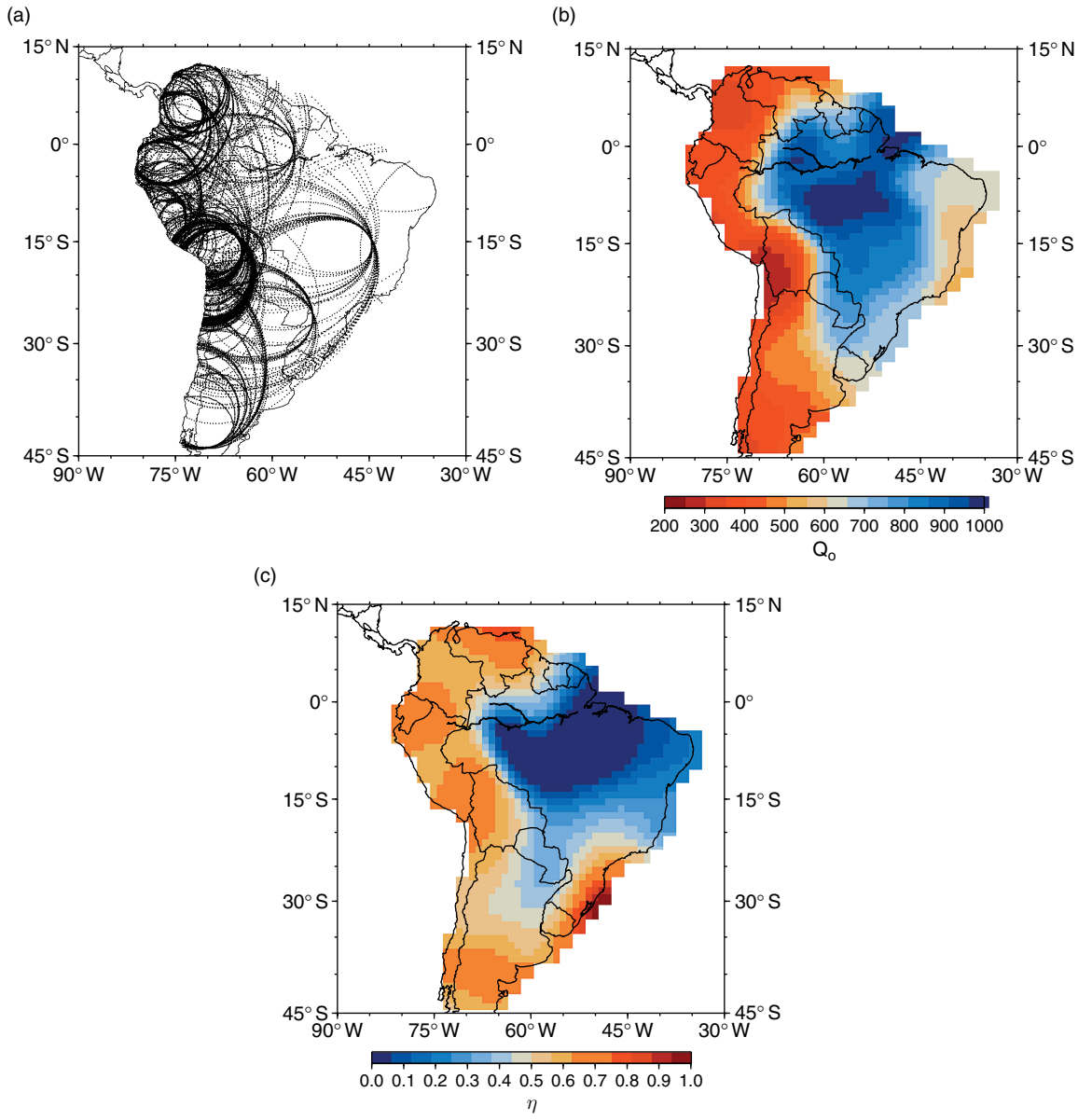

Figure 15 (a) A scattering ellipse map, (b) a Q_o map, and (c) an η map for South America. Adapted from DeSouza JL and Mitchell BJ (1998) *Lg* coda *Q* variations across South America and their relation to crustal evolution. *Pure and Applied Geophysics* 153: 587–612.

low Q_o lies in central Siberia and corresponds spatially to the Siberian Traps.

The four zones with lowest Q values lie in the Kamchatka Peninsula in northeastern Siberia, the southeastern portions of the Tibetan Plateau and Himalaya, the Hindu Kush (just north of India) and western Turkey. All of these regions are also highly seismically active, a correspondence that suggests that low-Q regions are associated with regions of high crustal strain.

Other low-Q regions appear to be related to upper mantle processes. A comparison of **Figure 13(b)** with wave velocities at long periods (Ekström *et al.*, 1997), that are not sensitive to crustal properties, shows a correspondence of low-Q regions with regions of low upper mantle velocities. This is most apparent for the broad band of low Q values throughout southern Eurasia but also occurs in the Siberian Trap region of Siberia. Both the low-Q and low-velocity regions largely coincide with high

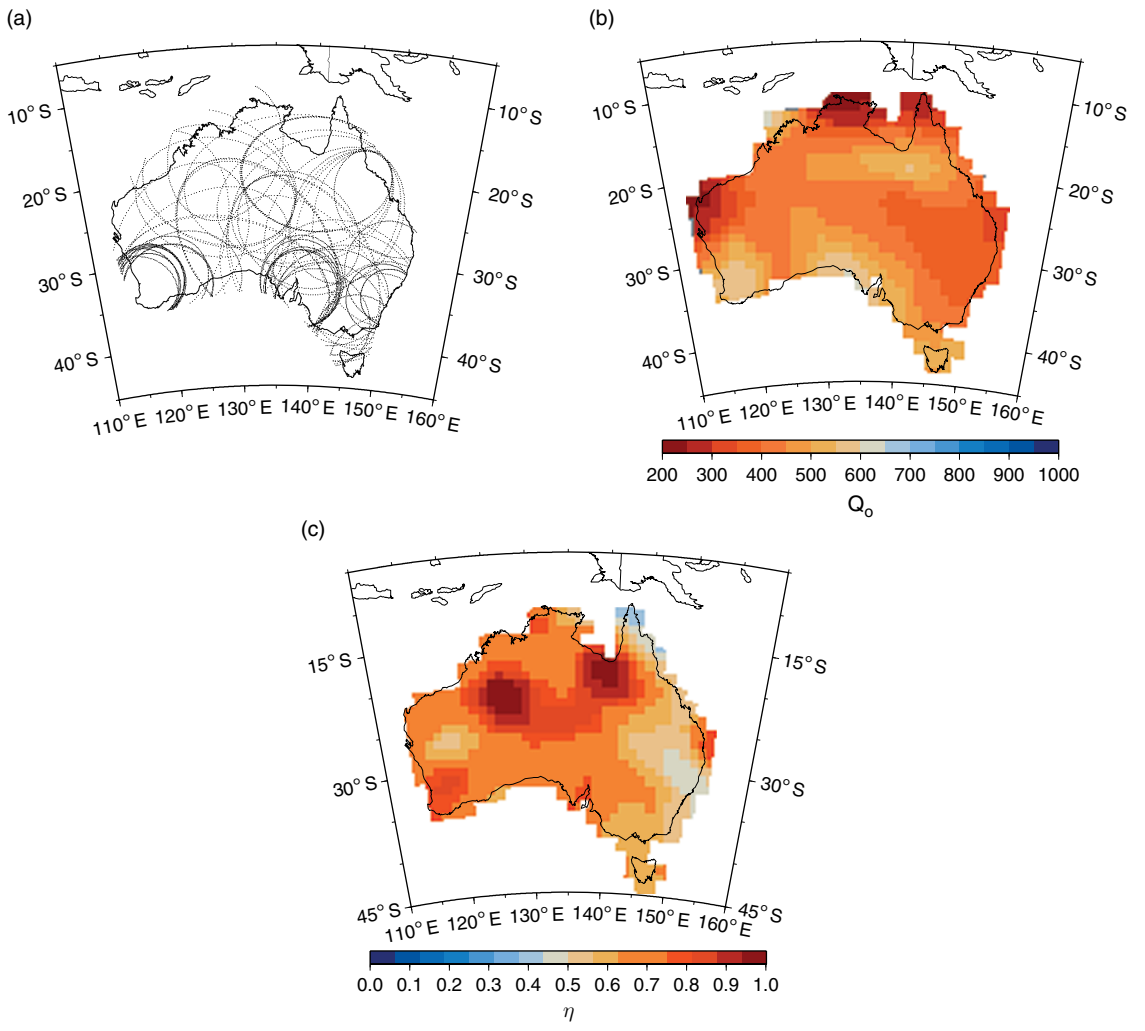

Figure 16 (a) A scattering ellipse map, (b) a Q_o map, and (c) an *eta* map of Q_{Lg}^{C} for Australia. Adapted from Mitchell BJ, Baqer S, Akinci A, Cong L (1998) *Lg* coda *Q* in Australia and its relation to crustal structure and evolution. *Pure and Applied Geophysics* 153: 639–653.

upper mantle temperatures (Artemieva and Mooney 2001).

Patterns of frequency dependence (η) variation in **Figure 13(c)**, in contrast to those of Q_o variation, show no clear-cut relationship to tectonics. They similarly show no relation to patterns of Q_o variation. For instance, Kamchatka has low Q_o and low η while Spain has low Q_o and high η.

Seismologists have performed other tomographic studies for portions of Eurasia using Q_{Lg} and shear-wave Q (Q_μ). Xie *et al.* (2006) used a two-station version of the SSR method to determine more than 5000 spectal ratios over 594 paths in eastern Eurasia. They were able to obtain tomographic models for Q_o and η with resolution ranging between 4° and 10° in which Q_o varies between 100 and 900.

Using the single-station multimode method (Cheng and Mitchell, 1981), Jemberie and Mitchell (2004) obtained tomographic maps of shear-wave Q (Q_μ) for depth ranges of 0–10 and 10–30 km. Although large standard errors accompany those determinations several features of their variation patterns, such as the low-Q regions in southern Tibet, resemble the map of Q_o variations (**Figure 13(b)**). Q_μ varies between about 30 and 280 in the upper 10 km of the crust and between about 30 and 180 at 10–30 km depth.

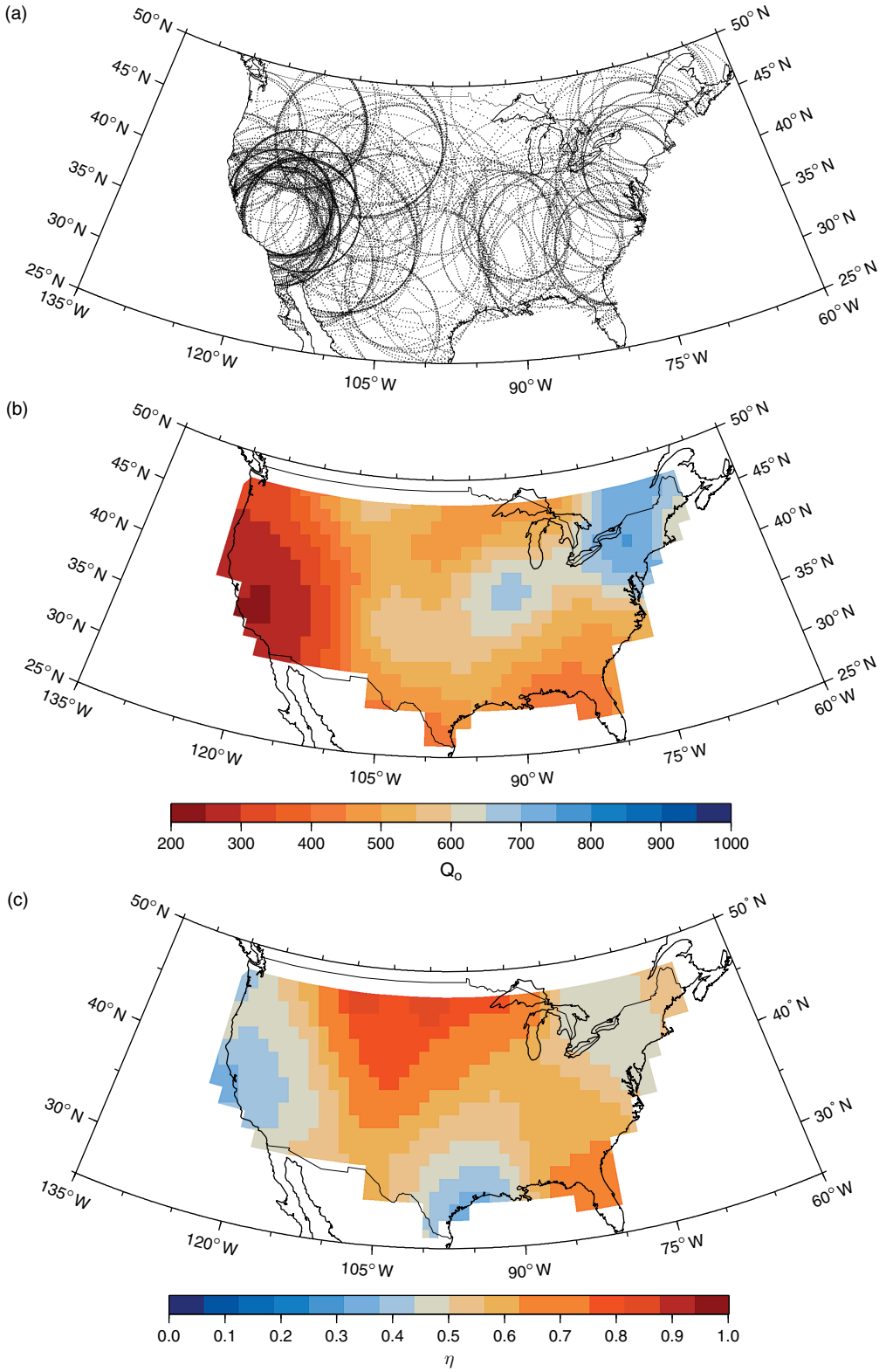

Figure 17 (a) A scattering ellipse map, (b) a Q_o map, and (c) an *eta* map of Q_{Lg}^{C} for the United States. Adapted from Baqer S and Mitchell BJ (1998) Regional variation of *Lg* coda *Q* in the continental United States and its relation to crustal structure and evolution. *Pure and Applied Geophysics* 153: 613–638.

1.21.7.3.2 Q^C_{Lg} tomography in Africa

Xie and Mitchell (1990b), in the first tomographic study of Lg coda, determined Q_o and η for continental Africa. **Figure 14** shows maps of data coverage, Q_o and η for that entire continent (Xie and Mitchell, 1990b). The features in the Q_o map (**Figure 14(b)**) that is most obviously related to tectonics is the low-Q region that broadly coincides with the East African Rift system. The three high-Q regions correspond to Precambrian cratons: the West African Craton in the northwest, the East Sahara Craton in the northeast, and the Kalahari Craton in the south. The Congo Craton, situated just to the north of the Kalahari Craton does not show up as a region of high Q, probably because waves are damped by a broad and deep basin of low-Q sedimentary rock in that region.

Low Q_o values also occur in the Atlas Mountains (Cenozoic age) of northern Africa, the Cape Fold Belt (Permo-Triassic age) at the southern tip of Africa and the Cameroon Line (Miocene age) which is oriented in an NNE–SSW direction from the point where the western coast changes direction from east–west to north–south.

1.21.7.3.3 Q^C_{Lg} and Q_{Lg} tomography in South America

Figure 15 shows data coverage, and values of Q_o and η obtained for South America (DeSouza and Mitchell, 1998). The data coverage (**Figure 15(a)**) is excellent throughout western South America where seismicity is high but poor in eastern regions, especially the most easterly regions, where there are few earthquakes. **Figure 15(b)** shows that, as expected, the low-Q (250–450) portion of South America is associated with the tectonically active western coastal regions. The lowest Q_o values occur along the coast between 15° and 25° S latitude where the level of intermediate-depth seismicity is highest in the continent. The slab in this region also dips steeply (>20°) and significant volcanism occurs (Chen *et al.*, 2001). Davies (1999) had studied the role of hydraulic fractures and intermediate-depth earthquakes in generating subduction zone magmatism. He suggested that the level of intermediate-depth earthquakes was high because liberated fluids favored brittle fracture in response to stresses acting on the slab. Q levels may be low there because earthquake activity creates a degree of permeability that allows dehydrated fluids to be transported to the mantle wedge.

Ojeda and Ottemöller (2002), developed maps of Lg attenuation for most of Colombia at various frequencies in the 0.5–5.0 Hz range. They delineated regional variations of Q_{Lg} within that relatively small region.

1.21.7.3.4 Q^C_{Lg} tomography in Australia

Figure 16 shows the data coverage and values of Q_o and η obtained for Australia (Mitchell *et al.*, 1998). Data coverage (**Figure 16(a)**) there was the poorest of the five continents where Q^C_{Lg} was mapped over continent-scale dimensions. Q_o variation there is consistent, however, with the other studies and, for all but peripheral regions where systematic measurement errors can be high, it displays a clear relationship with past tectonic activity. Q_o in Australia (**Figure 16(b)**) is unusually low for a stable continental region, perhaps because a velocity gradient rather than a sharp interface separates the crust and mantle.

Highest values range between 550 and 600 in the southeastern corner of the continent (the Yilgarn Block) and along the southern coast (the Gawler Block). Values between 400 and 500 characterize much of the remaining cratonic crust. This compares with values of 800 and higher in most of the African and South American cratons. The youngest crust lies in eastern Australia where Q_o is between 350 and 400. An orogeny occurred there during the Devonian Period and another occurred in the eastern portion of that region during the Permian Period. Low Q_o values in the most westerly point of the continent and along the northern coast are probably due to very poor data coverage there (**Figure 16(a)**) and are probably meaningless.

1.21.7.3.5 Q^C_{Lg}, Q_{Lg}, and P/S tomography in North America

Figure 17 shows the data coverage, Q_o, and η values obtained for the United States (Baqer and Mitchell, 1998). Coverage (**Figure 17(a)**) is best in the western portions of the country, but is also reasonably good in the central and eastern portions. **Figure 17(b)** shows that Q_o is lowest (250–300) in California and the Basin and Range Province. That low-Q region forms the core of a broader region low of Q_o values that extends approximately to the western edge of the Rocky Mountains. Q_o in the Rocky Mountains and much of the Great Plains ranges between about 450 and 600. A moderately high-Q (mostly 600–700) corridor extends from Missouri to the north Atlantic states and New

England. Q_o in New York and peripheral regions is somewhat higher (700–750). An earlier study of Q_{Lg} in the northeastern United States (Shi *et al.*, 1996) found Q_o and η values that are similar to the country-wide tomographically derived values in that region.

Two research groups have studied the 3-D structure of P-wave and S-wave attenuation in southern California. Schlotterbeck and Abers (2001) fit theoretical spectra to observed spectra using the least-square minimization method of Hough *et al.* (1988), and determined t^* for P- and S-waves at frequencies between 0.5 and 25 Hz. Their inversions showed that P and S results were in substantial agreement, that Q varies spatially and correlates with regional tectonics.

The second California study (Hauksson, 2006) also determined t^* from P- and S-wave spectra. They assumed that t^* consists of the sum of the whole-path attenuation and the local site effect at each recording station and utilized an expression of Eberhart-Phillips and Chadwick (2002) for the velocity spectrum. The inversion, in addition to providing t^*, yields parameters defining the velocity amplitude spectra. They determined t^* for about 340 000 seismograms from more than 5000 events of t^* data to obtain 3-D, frequency-independent crustal models for Q_P and Q_S in the crust and uppermost mantle in southern California. They found that both Q_P and Q_S generally increase with depth from values of 50 or less in surface sediments to 1000 and greater at mid-crustal depths. Their models reflect major tectonic structures to a much greater extent than they reflect the thermal structure of the crust. Al-Eqabi and Wysession (2006) conducted a tomographic study of Q_{Lg} in the Basin and Range province using a genetic algorithm technique. They found that Q_{Lg} increases (234–312) in a southwest–northeast direction across the Basin and Range in good agreement with the variation of Q_{Lg}^{C} reported by Baqer and Mitchell (1998). As part of a broader study of Lg wave propagation in southern Mexico Ottemöller *et al.* (2002) used formal inversion methods to separately obtain tomographic maps of Q_{Lg} at three frequencies (0.5, 2.0, and 5.0 Hz) using 1° by 1° cells. Because of uneven path coverage in southern Mexico they applied regularization conditions to their inversion equations. They found lower than average Q_{Lg} in the Gulf of Mexico coastal plain and the area east of 94° W, average values in the northern portion of the Pacific coastal region, and below average values in the southern portion.

1.21.7.3.6 Q_P variation near ocean ridges

Wilcock *et al.* (1995) developed a spectral technique by which they determined the attenuation of P waves in an active-source experiment centered at the East Pacific Rise at latitude 9° 30′ N. It is, to date, the only tomographic study of crustal Q variation in an oceanic region. They obtained over 3500 estimates of t^*, the path integral of the product of Q^{-1} and P-wave velocity where both quantities are variable along the path. Wilcock *et al.* display plots of both cross-axis as well as along-axis structure for upper crustal and lower crustal Q^{-1} structure. Within the ridge magma chamber Q reaches minimum values of 20–50 which extend to the base of the crust. Off the ridge axis they find that Q in the upper crust is 35–50 and at least 500–1000 at depths greater than 2–3 km.

1.21.7.3.7 Variation of crustal Q with time

Several investigators (e.g., Chouet, 1979; Jin and Aki, 1986) have reported temporal variations of Q over timescales of a few years. Although this observation has been reported several times, it continues to be controversial. Spatial patterns of Q variation and their apparent relation to time that has elapsed since the most recent episode of tectonic activity in any region, however, suggest that temporal variations of Q over very long periods of time can easily be detected. Mitchell and Cong (1998) found that variation for Q_{Lg}^{C} at 1 Hz extends between roughly 250, for broad regions that are currently tectonically active, and about 1000 for shields that have been devoid of tectonic activity for a billion years or more (**Figure 18**). Mitchell *et al.* (1997) explained those observations as being due to variable volumes of fluids in faulted, fractured, and permeable rock. Fluids may enhance the rate of attenuation of seismic waves either because the waves must expend energy to push those fluids through permeable rock as they propagate or they may traverse a region of enhanced scattering that causes loss of wave energy into the mantle. **Figure 18** points to an evolutionary process in which fluids are relatively abundant in tectonically active regions due to their generation by hydrothermal reactions at high temperatures. With time, fluids are gradually lost, either by migration to the Earth's surface or absorption due to retrograde metamorphism. This process causes low Q values early in the tectonic cycle and gradually increasing values at later times as the fluids dissipate.

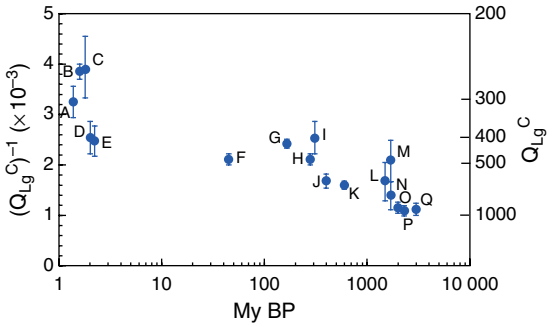

Figure 18 Q_o for Q_{Lg}^{C} at 1 Hz vs time elapsed in selected regions since the most recent episode of tectonic or orogenic activity. A, The Andes; B, Basin and Range Province in the western United States; C, Tethys region of convergence between the Eurasian and African/Arabian/Indian plates; D, The Arabian Peninsula; E, The East African Rift; F, The Rocky Mountains; G, northeastern China; H, The eastem Altaid belt in Eurasia; I, The Tasman Province in Australia; J, The Atlantic Shield in South America; K, The African fold belts; L, The portion of the North American Craton in the United States; M, The Australian Craton; N, Eurasian Cratons; O, African shields; P, The Brazilian shield; Q, The Indian shield. Adapted from Mitchell BJ and Cong L (1998) *Lg* coda *Q* and its relation to the structure and evolution of continents: A global perspective. *Pure and Applied Geophysics* 153: 655–663.

1.21.8 Conclusions

Much progress has been made in the last 10 years in characterizing the lateral variations of attenuation in the crust, especially under continents, and their relation to tectonics. Characterizing the nature and distribution of attenuation deeper in the Earth still remains a challenging subject, because of the persistent difficulties in separating anelastic and scattering effects, and the nonuniform sampling achieved with available data.

Still, it is encouraging to see that there is now consistency in the large-scale features of lateral variations in Q in the upper 200 km of the mantle and that accounting for focusing effects using a single scattering approximation in present-day elastic 3-D models is helpful, at least at the longest wavelengths. It is still important to consider that, when the inversion experiment is well designed, the unmodelled scattering effects can be minimized, or even utilized to constrain velocity models (e.g., Dalton and Ekström, 2006b), but the consequence is that significant damping needs to be applied in the inversion for lateral variations in Q. This results in large uncertainties (a factor of 2 or more) in the amplitudes of lateral variations of Q, so that physical interpretations of these models must remain tentative. On the other hand, the spatial distribution of low- and high-Q regions is, in general, more robust. Thus far, only one research group has produced models of lateral variations of Q_μ in the transition zone. While the results are consistent within this group using different methodologies (Romanowicz, 1995; Gung and Romanowicz, 2004) and point to an intriguing correlation with structure at the base of the mantle (Romanowicz and Gung, 2002), these results need to be confirmed by independent studies.

At the regional, uppermost mantle scale, a promising trend, made possible by improved data and techniques, is to combine attenuation, velocity, and other geophysical parameters to better constrain lateral variations of temperature and composition. An ambitious goal would be to do the same at the global, and deeper, scale. Progress in laboratory experiments on Q at seismic frequencies is just starting to provide reliable mineral physics parameters on the behavior of Q at depths down to the upper mantle low velocity zone, so that joint inversions of seismic waveform data for elastic and anelastic 3-D structure can be envisaged (e.g., Cammarano and Romanowicz, 2006). The challenge here is in the nonlinearities introduced by the exponential variation of Q with temperature, on the one hand, and the variation in the position of mineral phase changes depending on composition.

Important uncertainties remain in the characterization of the 1-D profile of Q_μ in the mantle. First and foremost, explaining once and for all the discrepancy between free oscillations and surface-wave measurements, which has consequences for the value of Q_μ in the transition zone. Because there are still unexplained discrepancies between elastic models of the upper mantle, and particularly the transition zone, produced from seismic data on the one hand, and from mineral physics data and computations, on the other (e.g., Cammarano *et al.*, 2003), it is particularly important to apply accurate anelastic corrections when interpreting seismic velocity models in terms of composition. The evidence for a maximum in Q_μ in the lower mantle, and therefore lower Q_μ at the base of the mantle, is now clear, however, the location of this maximum is not well constrained.

The presence of hemispherical variations in Q_α at the top of the inner core, the confirmation of increasing Q with depth and of anisotropy in Q_α correlated with anisotropy in velocity are exciting results that need further investigation, in particular in the light of recent studies by Li and Cormier (2002) favoring a scattering interpretation of attenuation in the inner core.

Finally, in the shallow Earth, it has been found over the past three decades that crustal Q_c as manifested by regional studies of body waves, Lg and Lg coda, varies tremendously across contients, as well as in average values of different continents. Q_o for Lg coda varies between about 150 and 1000 for features that can be resolved at 1 Hz frequency and the frequency dependence of Lg coda Q varies between about 0.0 and 1.0. Most Q determinations at short periods in any region appear to be governed, most prominently, by the time that has elapsed since the most recent episode of tectonic or orogenic activity there.

Acknowledgment

The research of BJM was partially supported by the Air Force Research Laboratory under Award FA 8718-04-C-0021.

References

Abercrombie RE (1997) Near-surface attenuation and site effects from comparison of surface and deep borehole recordings. *Bulletin of the Seismological Society of America* 87: 731–744.

Abercrombie RE (2000) Crustal attenuation and site effects at Parkfield, California. *Journal of Geophysical Research* 105: 6277–6286.

Aki K (1969) Analysis of the seismic coda of local earthquakes as scattered waves. *Journal of Geophysical Research* 74: 615–631.

Aki K (1980) Scattering and attenuation of shear waves in the lithosphere. *Journal of Geophysical Research* 85: 6496–6504.

Akopyan ST, Zharkov VN, and Lyubimov VM (1976) Corrections to the eigenfrequencies of the Earth due to dynamic shear modulus. *Bulletin of the Seismological Society of America* 12: 625–630.

Al-Eqabi GI and Wysession ME (2006) Q_{Lg} distribution in the Basin and Range province of the Western United States. *Bulletin of the Seismological Society of America* 96: 348–354.

Al-Khatib HH and Mitchell BJ (1991) Upper mantle anelasticity and tectonic evolution of the Western United States from surface wave attenuation. *Journal of Geophysical Research* 96: 18129–18146.

Al-Shukri HJ, Mitchell BJ, and Ghalib HAA (1988) Attenuation of seismic waves in the New Madrid seismic zone. *Seismological Research Letters* 59: 133–140.

Allen RM, Nolet G, Morgan WJ, *et al.* (1999) The thin hot plume beneath Iceland. *Geophysical Journal International* 137: 51–63.

Anderson DL and Archambeau CB (1966) The anelasticity of the Earth. *Journal of Geophysical Research* 69: 2071–2084.

Anderson DL, Ben-Menahem A, and Archambeau CB (1965) Attenuation of seismic energy in the upper mantle. *Journal of Geophysical Research* 70: 1441–1448.

Anderson DL and Given JW (1982) Absorption band Q model for the Earth. *Journal of Geophysical Research* 87: 3893–3904.

Anderson DL and Hart RS (1976) An Earth model based on free oscillations and body waves. *Journal of Geophysical Research* 81: 1461–1475.

Anderson DL and Hart RS (1978) Q of the Earth. *Journal of Geophysical Research* 83: 5869–5882.

Anderson JG and Hough SE (1984) A model for the shape of Fourier amplitude spectrum of acceleration at high frequencies. In: *1984 Annual Meeting*, 30 May–3 June, 1984. Anchorage, Alaska: Seismological Society of America.

Andrews J, Deuss A, and Woodhouse J (2006) Coupled normal mode sensitivity to inner-core shear velocity and attenuation. *Geophysical Journal International* 167: 204–212.

Angenheister GH (1906) Bestimmung der fortpflanzungsgeschwindigkeit und absorption von erdbebenwellen, die durch den gegenpunkt des Herdes gegangen sind. *Nachrichten von der Königlichen Gesellschaft der Wissenschaften zu Göttingen* 110–120.

Angenheister GH (1921) Beobachtungen an pazifischen beben. *Nachrichten von der Königlichen Gesellschaft der Wissenschaften zu Göttingen* 113–146.

Artemieva IM, Billien M, Lévêque JJ, and Mooney WD (2004) Shear-wave velocity, seisic attenuation, and thermal structure of the continental upper mantle. *Geophysical Journal International* 157: 607–628.

Artemieva IM and Mooney WD (2001) Thermal evolution of precambrian lithosphere: A global study. *Journal of Geophysical Research* 106: 16387–16414.

Asada T and Takano K (1963) Attenuation of short-period *P* waves in the mantle. *Journal of Physics of the Earth* 11: 25–34.

Baqer S and Mitchell BJ (1998) Regional variation of *Lg* coda *Q* in the continental United States and its relation to crustal structure and evolution. *Pure and Applied Geophysics* 153: 613–638.

Barazangi M and Isaaks B (1971) Lateral variations of seismic-wave attenuation in the upper mantle above the inclined earthquake zone of the Tonga Island Arc: Deep anomaly in the upper mantle. *Journal of Geophysical Research* 76: 8493–8516.

Barazangi M, Pennington W, and Isaaks B (1975) Global study of seismic wave attenuation in the upper mantle behind Island Arcs using P waves. *Journal of Geophysical Research* 80: 1079–1092.

Ben-Menahem A (1965) Observed attenuation and Q values of seismic surface waves in the upper mantle. *Journal of Geophysical Research* 70: 4641–4651.

Benz HM, Frankel A, and Boore DM (1997) Regional *Lg* attenuation for the continental United States. *Bulletin of the Seismological Society of America* 87: 606–619.

Bhattacharyya J, Masters G, and Shearer P (1996) Global lateral variations of shear wave attenuation in the upper mantle. *Journal of Geophysical Research* 101: 22273–22289.

Bhattacharyya J, Shearer P, and Masters G (1993) Inner core attenuation from short period *PKP*(*BC*) versus *PKP*(*DF*) waveforms. *Geophysical Journal International* 114: 1–11.

Billien M and Lévêque J (2000) Global maps of Rayleigh wave attenuation for periods between 40 and 150 seconds. *Geophysical Research Letters* 27: 3619–3622.

Bollinger GA (1979) Attenuation of the *Lg* phase and determination of m_b in thee Southeastern United States. *Bulletin of the Seismological Society of America* 69: 45–63.

Bolt BA (1977) The detection of PKIIKP and damping in the inner core. *Annali di Geofisica* 30: 507–520.

Bowers (2000) Observations of PKP(DF) and PKP(BC) across the United Kingdom: Implications for studies of attenuation in the Earth's core. *Geophysical Journal International* 140: 374–384.

Bowman RJ (1988) Body wave attenuation structure in the Tonga subduction zone. *Journal of Geophysical Research* 93: 2125–2139.

Bowman JR and Kennett BLN (1991) Propagation of *Lg* waves in the North Australian craton: Influence of crustal velocity gradients. *Bulletin of the Seismological Society of America* 81: 592–610.

Boyd OS and Sheehan AF (2005) Attenuation tomography beneath the rocky mountain front: Implications for the physical state of the upper mantle. In: Karlstrom KE and Keler GR (eds.) *Geophysical Monograph Series 154*: *The Rocky Montain Region: An evolving lithosphere*, pp. 361–377. Washington, DC: American Geophysical Union.

Brune JN (1970) Tectonic stress and the spectra of seismic shear waves from earthquakes. *Journal of Geophysical Research* 75: 4997–5009.

Buland R and Gilbert F (1978) Improved resolution of complex eigenfrewquencies in analytically continued seismic spectra. *Geophysical Journal of the Royal Astronomical Society* 52: 457–470.

Cammarano F, Goes S, Vacher P, and Giardini D (2003) Inferring upper-mantle temperatures from seismic velocities. *Physics of the Earth and Planetary Interiors* 138: 197–222.

Cammarano F and Romanowicz B (2006) Insights into the nature of the transition zone from physically constrained inversion of long period seismic data. *Physics of the Earth and Planetary Interiors* 138: 197–222.

Campillo M, Plantet JL, and Bouchon M (1985) Frequency-dependent attenuation in the crust beneath central France from *Lg* waves: Data analysis and numerical modeling. *Bulletin of the Seismological Society of America* 75: 1395–1411.

Canas JA and Mitchell BJ (1978) Lateral variation of surface-wave anelastic attenuation across the Pacific. *Bulletin of the Seismological Society of America* 68: 1637–1650.

Canas JA and Mitchell BJ (1981) Rayleigh-wave attenuation and its variation across the Atlantic Ocean. *Geophysical Journal of the Royal Astronomical Society* 67: 159–176.

Cao A (2005) *Seismological Constraints on Inner Core Properties*. PhD Dissertation, University of California at Berkeley, Berkeley, CA.

Cao A and Romanowicz B (2004) Hemispherical transition of seismic attenuation at the top of the Earth's inner core. *Earth and Planetary Science Letters* 228: 243–253.

Cao A, Romanowicz B, and Takeuchi N (2005) An observation of *PKJKP*: Inferences on inner core shear properties. *Science* 308: 1453–1455.

Carcione JM and Cavallini F (1995) A rheological model for anelastic anisotropic media with applications to seismic wave propagation. *Geophysical Journal International* 119: 338–348.

Carpenter PJ and Sanford AR (1985) Apparent Q for upper crustal rocks of the central Rio Grande Rift. *Journal of Geophysical Research* 90: 8661–8674.

Chan WW and Der ZA (1988) Attenuation of multiple *ScS* in various parts of the world. *Geophysical Journal International* 92: 303–314.

Chavez D and Priestley KF (1986) Measurement of frequency dependent *Lg* attenuation in the Great Basin. *Geophysical Research Letters* 60: 551–554.

Chen PF, Bina CR, and Okal EA (2001) Variations in slab dip along the subducting Nazca plate, as related to stress patterns and moment release of intermediate-depth seismicity and to surface volcanism. *Geochemistry Geophysics Geosystems* 2, doi:10.1029/2001GC000,153.

Cheng HX and Kennett BLN (2002) Frequency dependence of seismic wave attenuation in the upper mantle in the Australian region. *Geophysical Journal International* 150: 45–47.

Cheng CC and Mitchell BJ (1981) Crustal *Q* structure in the United States from multi-mode surface waves. *Bulletin of the Seismological Society of America* 71: 161–181.

Chouet B (1979) Temporal variation in the attenuation of earthquake coda near Stone Canyon, California. *Geophysical Research Letters* 6: 143–146.

Choy G and Cormier VF (1983) The structure of the inner core inferred from short-period and broadband GDSN data. *Geophysical Journal International* 63: 457–470.

Chun KY, West GF, Kikoski RJ, and Samson C (1987) A novel technique for measuring *Lg* attenuation – Results from eastern Canada between 1-Hz and 10-Hz. *Bulletin of the Seismological Society of America* 77: 398–419.

Cong L and Mitchell BJ (1998) Seismic velocity and *Q* structure of the middle eastern crust and upper mantle from surface-wave dispsersion and attenuation. *Pure and Applied Geophysics* 153: 503–538.

Cormier VF (1981) Short period *PKP* pahses and the anelastic mechanism of the inner core. *Physics of the Earth and Planetary Interiors* 24: 291–301.

Cormier VF and Li X (2002) Frequency-dependent seismic attenuation in the inner core. Part 2: A scattering and fabric interpretation. *Journal of Geophysical Research* 107, doi:10.1029/2002JB001,796.

Cormier VF and Richards P (1976) Comments on the damping of core waves by Anthony Qamar and Alfredo Eisenberg. *Journal of Geophysical Research* 81: 3066–3068.

Cormier VF and Richards P (1988) Spectral synthesis of body waves in Earth models specified by vertically varying layers. In: Doornbos D (ed.) *Seismological Algorithms*, pp. 3–45. San Diego, CA: Academic Press.

Cormier VF and Stroujkova A (2006) Waveform search for the innermost inner core. *Earth and Planetary Science Letters* 236: 96–105.

Cormier VF, Xu L, and Choy GL (1998) Seismic attenuation of the inner core: Viscoelastic or stratigraphic? *Geophysical Research Letters* 25: 4019–4022.

Creager KC (1992) Anisotropy of the inner core from differential travel times of the phases *PKP* and *PKIKP*. *Nature* 356: 309–314.

Creager KC (1999) Large-scale variations in inner core anisotropy. *Journal of Geophysical Research* 104: 23127–23139.

Dainty AM (1981) A scattering model to explain *Q* observations in the lithosphere between 1 and 30 Hz. *Geophysical Research Letters* 8: 1126–1128.

Dalton C and Ekström G (2006a) Constraints on global maps of phase velocity from surface-wave amplitudes. *Geophysical Journal International* 167: 820–826.

Dalton C and Ekström G (2006b) Global models of surface wave attenuation. *Journal of Geophysical Research* 111, doi:10.1029/2005JB003,997.

Davies JH (1990) Mantle plumes, mantle stirring and hotspot geometry.

Davies JH (1999) The role of hydraulic fractures and intermediate-depth earthquakes in generating subduction-zone magmatism. *Nature* 398: 142–145.

Der ZA, McElfresh TW, and O Donnell A (1982) An investigation of the regional variations and frequency dependence of anelastic attenuation in the mantle under the United States in the 0.5-4 Hz band. *Geophysical Journal of the Royal Astronomical Society* 69: 67–99.

Deschamps A (1977) Inversion of the attenuation data of free oscillations of the Earth (fundamental and first higher modes). *Geophysical Journal of the Royal Astronomical Society* 50: 699–722.

DeSouza JL and Mitchell BJ (1998) *Lg* coda *Q* variations across South America and their relation to crustal evolution. *Pure and Applied Geophysics* 153: 587–612.

Ding CY and Grand SP (1993) Upper mantle Q structure under the East Pacific Rise. *Journal of Geophysical Research* 98: 1973–1975.

Doornbos DJ (1974) The anelasticity of the inner core. *Geophysical Journal of the Royal Astronomical Society* 38: 397–415.

Doornbos DJ (1983) Observable effects of the seismic absorption band in the Earth. *Geophysical Journal of the Royal Astronomical Society* 57: 381–395.

Durek JJ and Ekström G (1995) Evidence for bulk attenuation in the asthenosphere from recordings of the Bolia earthquake. *Geophysical Research Letters* 22: 2309–2312.

Durek JJ and Ekström G (1996) A radial model of anelasticity consistent with long-period surface wave attenuation. *Bulletin of the Seismological Society of America* 86: 144–158.

Durek JJ and Ekström G (1997) Investigating discrepancies among measurements of traveling and standing wave attenuation. *Journal of Geophysical Research* 102: 24529–24544.

Durek JJ, Ritzwoller MH, and Woodhouse JH (1993) Constraining upper mantle anelasticity using surface wave amplitude anomalies. *Geophysical Journal International* 114: 249–272.

Dziewonski AM and Anderson DL (1981) Preliminary reference Earth model. *Physics of the Earth and Planetary Interiors* 25: 297–356.

Dziewonski AM and Steim JM (1982) Dispersion and attenuation of mantle waves through waveform inversion. *Geophysical Journal of the Royal Astronomical Society* 70: 503–527.

Eberhart-Phillips D and Chadwick M (2002) Three-dimensional attenuation model of the shallow Hikurangi subduction zone in the Raukumara Peninsula, New Zealand. *Journal of Geophysical Research* 107: 2033 (doi:10.1029/2000JB000,046).

Ekström G and Dziewonski AM (1997) The unique anisotropy of the Pacific upper mantle. *Nature* 394: 168–172.

Ekström G, Tromp J, and Larson EWF (1997) Measurements and global models of surface wave propagation. *Journal of Geophysical Research* 102: 8137–8157.

Evernden JF (1955) Tripartite results for the Kamchatka earthquake of November 4, 1952. *Bulletin of the Seismological Society of America* 45: 167–178.

Faul U, FitzGerald J, and Jackson I (2004) Shear wave attenuation and dispersion in melt-bearing olivine polycrystals. Part 2: Microstructural interpretation and seismological implications. *Journal of Geophysical Research* 109, doi:10.1029/2003JB002,407.

Faul U and Jackson I (2005) The seismological signature of temperature and grain size variations in the upper mantle. *Earth and Planetary Science Letters* 234: 119–134.

Fearn DR, Loper DE, and Roberts PH (1981) Structure of the Earth's inner core. *Nature* 292: 232–233.

Fisher JL and Wysession ME (2003) Small-scale lateral variations in D'' attenuation and velocity structure. *Geophysical Research Letters* 30, doi:10.1029/2002GL016,179.

Flanagan MP and Wiens DA (1990) Attenuation structure beneath the Lau back arc spreading center from teleseismic S phases. *Geophysical Research Letters* 17: 2117–2120.

Flanagan MP and Wiens DA (1994) Radial upper mantle structure of inactive back-arc basins from differential shear wave measurements. *Journal of Geophysical Research* 99: 15469–15485.

Flanagan MP and Wiens DA (1998) Attenuation of broadband P and S waves in Tonga; observations of frequency dependent Q. *Pure and Applied Geophysics* 153: 345–375.

Frankel A and Wennerberg L (1987) Energy-flux model for seismic coda: Separation of scattering and intrinsic attenuation. *Bulletin of the Seismological Society of America* 77: 1223–1251.

Futterman A (1962) Dispersive body waves. *Journal of Geophysical Research* 67: 5279–5291.

Garcia R (2002) Constraints on upper inner-core structure from waveform inversion of core phases. *Geophysical Journal International* 150: 651–664.

Geller RJ and Stein S (1978) Time domain measurements of attenuation of fundamental modes (${}_0S_6 - {}_0S_{28}$). *Bulletin of the Seismological Society of America* 69: 1671–1691.

Getting IC, Dutton SJ, Burnley PC, Karato SI, and Spetzler HA (1997) Shear attenuation and dispersion in MgO. *Physics of the Earth and Planetary Interiors* 99: 249–257.

Giardini DXDL and Woodhouse JH (1988) Splitting functions of long period normal modes of the Earth. *Journal of Geophysical Research* 93: 13716–13742.

Gilbert F and Dziewonski AM (1975) An application of normal mode theory to the retrieval of structural parameters and source mechanisms from seismic spectra. *Philosophical Transactions of the Royal Society of London Series A* 278: 187–269.

Gomer BM and Okal EA (2003) Multiple-ScS probing of the Ontong-Java Plateau. *Physics of the Earth and Planetary Interiors* 138: 317–331.

Gueguen Y, Darot M, Mazot P, and Woirgard J (1989) Q^{-1} of forsterite single crystals. *Physics of the Earth and Planetary Interiors* 55: 254–258.

Gung Y, Panning M, and Romanowicz BA (2003) Anisotropy and thickness of the lithosphere. *Nature* 422: 707–711.

Gung Y and Romanowicz BA (2004) Q tomography of the upper mantle using three component long period waveforms. *Geophysical Journal International* 157: 813–830.

Gusev AA and Abubakirov IR (1996) Simulated envelopes of non-isotropically scattered body waves as copared to observed ones: Another manifestion of fractal inhomogeneity. *Geophysical Journal International* 127: 49–60.

Gutenberg B (1924) Dispersion und extinktion von seismischen oberflächenwellen und der aufbau der obersten erdschichten. *Physikalische Zeitschrift* 25: 377–381.

Gutenberg B (1945a) Amplitudes of *P*, *PP*, and *SS* and magnitude of shallow earthquakes. *Bulletin of the Seismological Society of America* 35: 57–69.

Gutenberg B (1945b) Amplitudes of surface waves and magnitudes of shallow earthquakes. *Bulletin of the Seismological Society of America* 35: 3–12.

Gutenberg B (1958) Attenuation of seismic waves in the Earth's mantle. *Bulletin of the Seismological Society of America* 48: 269–282.

Hasegawa HS (1974) Theoretical synthesis and analysis of strong motion spectra of earthquakes. *Canadian Geotechnical Journal* 11: 278–297.

Hasegawa HS (1985) Attenuation of *Lg* waves in the Canadian shield. *Bulletin of the Seismological Society of America* 75: 1569–1582.

Hauksson E (2006) Attenuation models (Q_P and Q_S) in three dimensions of the Southern California crust: Inferred fluid saturation at seismogenic depths. *Journal of Geophysical Research* 111(B05): 302 (doi:10.129/2005JB003,947).

He X and Tromp J (1996) Normal-mode constraints on the structure of the Earth. *Journal of Geophysical Research* 101: 20053–20082.

Helffrich G, Kaneshima S, and Kendall JM (2002) A local, crossing-path study of attenuation and anisotropy of the inner core. *Geophysical Research Letters* 29, doi:10.1029/2001GL014,059.

Herrmann RB (1980) *Q* estimates using the coda of local earthquakes. *Bulletin of the Seismological Society of America* 70: 447–468.

Herrmann RB and Mitchell BJ (1975) Statistical analysis and interpretation of surface-wave anelastic attenuation data for the stable interior of North America. *Bulletin of the Seismological Society of America* 65: 1115–1128.

Hough SE, Anderson JG, Brune J, *et al.* (1988) Attenuation near Anza, California. *Bulletin of the Seismological Society of America* 78: 672–691.

Hough SE, Lees JM, and Monastero F (1999) Attenuation and source properties at the Coso geothermal area, California. *Bulletin of the Seismological Society of America* 89: 1606–1619.

Humphreys E and Clayton RW (1988) Adaptation of back projection tomography to seismic travel time problems. *Journal of Geophysical Research* 93: 1073–1086.

Hwang HJ and Mitchell BJ (1987) Shear velocities, Q_β, and the frequency dependence of Q_β in stable and tectonically active regions from surface wave observations. *Geophysical Journal of the Royal Astronomical Society* 90: 575–613.

Ichikawa M and Basham PW (1965) Variations in short-period records from Canadian seismograph stations. *Canadian Journal of Earth Sciences* 2: 510–542.

Isse T and Nakanishi I (1997) The effect of the crust on the estimation of mantle Q from spectral ratios of multiple ScS phases. *Bulletin of the Seismological Society of America* 87: 778–781.

Ivan M, Marza V, de Farias Caixeta D, and de Melo Arraes T (2005) Uppermost inner core attenuation from PKP data at South American seismological stations. *Geophysical Journal International* 164: 441–448.

Jackson I (1993) Progress in the experimental study of seismic wave attenuation. *Annual Review of Earth and Planetary Sciences* 21: 375–406.

Jackson I (2000) Laboratory measurement of seismic wave dispersion and attenuation: Recent progress. *Journal of Geophysical Research* 109, doi:10.1029/2003JB002,406.

Jackson I, Faul UH, Fitzgerald JD, and Tan BH (2004) Shear wave attenuation and dispersion in melt-bearing olivine polycrystals. Part 1: Specimen fabrication and mechanical testing. In: Karato S-I, Forte AM, Liebermann RC, Masters G, and Stixrude L (eds.) *Geophysical Monograph Series 117*: *Earth's Deep Interior*: *Mineral Physics and Tomography from the Atomic to the Global Scale*, pp. 265–289. Washington, DC: American Geophysical Union.

Jeffreys H (1967) Radius of the Earth's core. *Nature* 215: 1365–1366.

Jemberie AL and Mitchell BJ (2004) Shear-wave *Q* structure and its lateral variation in the crust of China and surrounding regions. *Geophysical Journal International* 157: 363–380.

Jin A and Aki K (1986) Temporal change in coda *Q* before the Tangshan earthquake of 1976 and the Haicheng earthquake of 1975. *Journal of Geophysical Research* 91: 665–673.

Jobert N and Roult G (1976) Periods and damping of free oscillations observed in France after 16 earthquakes. *Geophysical Journal of the Royal Astronomical Society* 45: 155–176.

Jordan TH and Sipkin SS (1977) Estimation of the attenuation operator for multiple ScS waves. *Geophysical Research Letters* 4: 167–170.

Kanamori H (1970) Velocity and Q of mantle waves. *Physics of the Earth and Planetary Interiors* 2: 259–275.

Kanamori H and Anderson DL (1977) Importance of physical dispersion in surface-wave and free oscillation problems. *Reviews of Geophysics* 15: 105–112.

Karato SI (1993) Importance of anelasticity in the interpretation of seismic tomography. *Geophysical Research Letters* 20: 1623–1626.

Karato SI (1998) A dislocation model of seismic wave attenuation and micro-creep in the Earth; Harold Jeffreys and the rheology of the solid Earth. *Pure and Applied Geophysics* 153: 239–256.

Karato SI and Karki BB (2001) Origin of lateral variation of seismic wave velocities and density in the deep mantle. *Journal of Geophysical Research* 106: 21771–21783.

Karato SI and Spetzler H (1990) Defect microdymamics in minerals and solid state mechanisms of seismic wave attenuation and velocity dispersion in the mantle. *Reviews of Geophysics* 28: 399–421.

Kijko A and Mitchell BJ (1983) Multimode Rayleigh wave attenuation and Q_β in the crust of the Barents shelf. *Journal of Geophysical Research* 88: 3315–3328.

Knopoff L (1964) *Q*. *Reviews of Geophysics* 2: 625–660.

Komatitsch D, Ritsema J, and Tromp J (2002) The spectral-element method, Beowulf computing, and global seismology. *Science* 298: 1737–1742.

Kovach RL and Anderson DL (1964) Attenuation of shear waves in the upper and lower mantle. *Bulletin of the Seismological Society of America* 54: 1855–1864.

Krasnoshchekov DN, Kaazik PB, and Ovtchinnikov VM (2005) Seismological evidence for mosaic structure of the surface of the Earth's inner core. *Nature* 435: 483–487.

Kumazawa M, Imanashi Y, Fukao Y, Furumoto M, and Yananoto A (1990) A theory of spectral analysis based on the characteristic property of a linear dynamical system. *Geophysical Journal International* 101: 613–630.

Kuster GT (1972) *Seismic Wave Propagation in Two-Phase Media and Its Application to the Earth's Interior.* PhD Dissertation, MIT, Cambridge, MA.

Lawrence JF, Shearer P, and Masters G (2006) Mapping attenuation beneath North America using waveform cross-correlation and cluster analysis. *Geophysical Research Letters* 33, doi:10.1029/2006GL025,813.

Lawrence JF and Wysession ME (2006) QLM9: A new radial quality factor (Q_{mu}) model for the lower mantle. *Earth and Planetary Science Letters* 241: 962–971.

Lay T and Kanamori H (1985) Geometric effects of global lateral heterogeneity on long-period surface wave propagation. *Journal of Geophysical Research* 90: 605–621.

Lay T and Wallace T (1983) Multiple ScS travel times and attenuation beneath Mexico and Central America. *Geophysical Research Letters* 10: 301–304.

Lay T and Wallace T (1988) Multiple ScS attenuation and travel times beneath Western North America. *Bulletin of the Seismological Society of America* 78: 2041–2061.

Lee WB and Solomon SC (1979) Simultaneous inversion of surface-wave phase velocity and attenuation: Rayleigh and Love waves over continental and oceanic paths. *Bulletin of the Seismological Society of America* 69: 65–95.

Li XD (1990) *Asphericity of the Earth from Free Oscillations*. PhD Dissertation, Harvard University, Cambridge, MA.

Li X and Cormier VF (2002) Frequency-dependent seismic attenuation in the inner core. Part 1: A viscoelastic interpretation. *Journal of Geophysical Research* 107, doi:10.1029/2002JB001,795.

Li XD and Romanowicz B (1995) Comparison of global waveform inversions with and without considering cross branch coupling. *Geophysical Journal International* 121: 695–709.

Liu HP, Anderson DL, and Kanamori H (1976) Velocity dispersion due to anelasticity: Implication for seismology and mantle composition. *Geophysical Journal of the Royal Astronomical Society* 47: 41–58.

Lognonné P and Romanowicz B (1990) Modelling of coupled normal modes of the Earth: The spectral method. *Geophysical Journal International* 102: 365–395.

Lomnitz C (1957) Linear dissipation in solids. *Journal of Applied Physics* 28: 201–205.

Loper DE and Fean DR (1983) A seismic model of a partially molten inner core. *Journal of Geophysical Research* 88: 1235–1242.

Loper DE and Roberts PH (1981) A study of conditions at the inner core boundary of the Earth. *Physics of the Earth and Planetary Interiors* 24: 302–307.

Luh P (1974) Normal modes of a rotating, self gravitating inhomogeneous Earth. *Geophysical Journal of the Royal Astronomical Society* 38: 187–224.

Lundquist GM and Cormier VC (1980) Constraints on the absorption band model of Q. *Journal of Geophysical Research* 85: 5244–5256.

Malin PE (1978) *A First Order Scattering Solution for Modeling Lunar and Terrestrial Seismic Coda*. PhD Dissertation, Princeton University, Princeton, NJ.

Masters G and Gilbert F (1981) Structure of the inner core inferred from observations of its spheroidal shear modes. *Geophysical Research Letters* 8: 569–571.

Masters G and Gilbert F (1983) Attenuation in the Earth at low frequencies. *Philosophical Transactions of the Royal Society of London Series XI* 308: 479–522.

Masters G and Laske G (1997) On bias in surface wave and free oscillation attenuation measurements. *Eos Transaction of the American Geophysical Union* 78: F485.

Mills J and Hales A (1978) Great circle Rayleigh wave attenuation and group velocity. Part III: Inversion of global average group velocity and attenuation coefficients. *Physics of the Earth and Planetary Interiors* 17: 307–322.

Minster B and Anderson DL (1981) A model of dislocation controlled rheology for the mantle. *Philosophical Transactions of the Royal Society of London Series A* 299: 319–356.

Mitchell BJ (1973) Radiation and attenuation of Rayleigh waves from the Southeastern Missouri earthquake of October 21, 1965. *Journal of Geophysical Research* 78: 886–899.

Mitchell BJ (1975) Regional Rayleigh wave attenuation on North America. *Journal of Geophysical Research* 35: 4904–4916.

Mitchell BJ (1995) Anelastic structure and evolution of the continental crust and upper mantle from seismic surface wave attenuation. *Reviews of Geophysics* 33: 441–462.

Mitchell BJ, Baqer S, Akinci A, and Cong L (1998) *Lg* coda *Q* in Australia and its relation to crustal structure and evolution. *Pure and Applied Geophysics* 153: 639–653.

Mitchell BJ and Cong L (1998) *Lg* coda *Q* and its relation to the structure and evolution of continents: A global perspective. *Pure and Applied Geophysics* 153: 655–663.

Mitchell BJ, Cong L, and Ekström G (2007) A continent-wide 1-Hz map of *Lg* coda *Q* variation across Eurasia and its implications for lithospheric evolution. *Journal of Geophysical Research* (in review).

Mitchell BJ and Helmberger DV (1973) Shear velocities at the base of the mantle from observations of *S* and *ScS*. *Journal of Geophysical Research* 78: 6009–6020.

Mitchell BJ and Hwang HJ (1987) The effect of low-*Q* sediments and crustal *Q* on *Lg* attenuation in the United States. *Bulletin of the Seismological Society of America* 77: 1197–1210.

Mitchell BJ, Pan Y, Xie J, and Cong L (1997) *Lg* coda *Q* across Eurasia and its relation to crustal evolution. *Journal of Geophysical Research* 102: 22767–22779.

Mitchell BJ and Xie J (1994) Attenuation of multiphase surface waves in the Basin and Range province. Part III: Inversion for crustal anelasticity. *Geophysical Journal International* 116: 468–484.

Modiano T and Hatzfeld D (1982) Experimental study of the spectral content for shallow earthquakes. *Bulletin of the Seismological Society of America* 72: 1739–1758.

Molnar P and Oliver J (1969) Lateral variations in attenuation in the upper mantle and discontinuities in the lithosphere. *Journal of Geophysical Research* 74: 2648–2682.

Montagner JP and Kennett BLN (1996) How to reconcile body-wave and normal-mode reference Earth models. *Geophysical Journal International* 125: 229–248.

Montagner JP and Tanimoto T (1991) Global upper mantle tomography of seismic velocities and anisotropy. *Journal of Geophysical Research* 96: 20337–20351.

Morelli A, Dziewonski AM, and Woodhouse JH (1986) Anisotropy of the core inferred from PKIKP travel times. *Geophysical Research Letters* 13: 1545–1548.

Mueller G (1986) Rheological properties and velocity dispersion of a medium with power law dependence of Q in frequency. *Journal of Geophysics* 54: 20–29.

Nakanishi I (1978) Regional differences in the phase velocity and the quality factor Q of mantle Rayleigh waves. *Science* 200: 1379–1381.

Nakanishi I (1979a) Attenuation of multiple ScS waves beneath the Japanese Arc. *Physics of the Earth and Planetary Interiors* 19: 337–347.

Nakanishi I (1979b) Phase velocity and Q of mantle Rayleigh waves. *Geophysical Journal of the Royal Astronomical Society* 58: 35–59.

Nakanishi I (1981) Shear velocity and shear attenuation models inverted from the worldwide and pure-path average data of mantle Rayleigh waves ($_0S_{25}$ to $_0S_{80}$) and fundamental spheroidal modes ($_0S_2$ to $_0S_{24}$). *Geophysical Journal of the Royal Astronomical Society* 66: 83–130.

Niazi M and Johnson LR (1992) Q in the inner core. *Physics of the Earth and Planetary Interiors* 74: 55–62.

Niu F and Wen L (2001) Hemispherical variations in seismic velocity at the top of the Earth's inner core. *Nature* 410: 1081–1084.

Nuttli OW (1973) Seismic wave attenuation and magnitude relations for Eastern North America. *Journal of Geophysical Research* 78: 876–885.

Nuttli OW (1978) A time-domain study of the attenuation of 10-Hz waves in the New Madrid seismic zone. *Bulletin of the Seismological Society of America* 68: 343–355.

Nuttli OW (1980) The excitation and attenuation of seismic crustal phases in Iran. *Bulletin of the Seismological Society of America* 70: 469–484.

O'Connell RJ and Budiansky B (1978) Measures of dissipation in viscoelastic media. *Geophysical Research Letters* 5: 5–8.

Ojeda A and Ottemöller L (2002) Q_{Lg} tomography in Colombia. *Physics of the Earth and Planetary Interiors* 130: 253–270.

Okal EA and Jo BG (2002) *Q* measurements for Phase X overtones. *Pure and Applied Geophysics* 132: 331–362.

Oki S, Fukao Y, and Obayashi M (2000) Reference frequency of teleseismic body waves. *Journal of Geophysical Research* 109, (doi:10.1029/2003JB002821).

Oreshin SI and Vinnik LP (2004) Heterogeneity and anisotropy of seismic attenuation in the inner core. *Geophysical Research Letters* 31, doi:10.1029/2003GL018,591.

Ottemöller L, Shapiro NM, Singh SK, and Pacheco JF (2002) Lateral variation of *Lg* wave propagation in southern Mexico. *Journal of Geophysical Research* 107(B1): 2008 (doi:10.1029/2001JB000,206).

Park J (1987) Asymptotic coupled-mode expressions for multiplet amplitude anomalies and frequency shift on a laterally heterogeneous Earth. *Geophysical Journal of the Royal Astronomical Society* 90: 129–170.

Patton HJ and Taylor SR (1989) *Q* structure of the Basin and Range from surface waves. *Journal of Geophysical Research* 89: 6929–6940.

Peacock S and Hudson JA (1990) Seismic properties of rocks with distributions of small cracks. *Geophysical Journal International* 102: 471–484.

Phillips S, Hartse HE, Taylor SR, and Randall GE (2000) 1 Hz Lg Q Tomography in central Asia. *Geophysical Research Letters* 27: 3425.

Press F (1956) Rigidity of the Earth's core. *Science* 124: 1204.

Randall MJ (1976) Attenuative dispersion and frequency shifts of the Earth's free oscillations. *Physics of the Earth and Planetary Interiors* 12: P1–P4.

Reid FJL, Woodhouse JH, and van Heist H (2001) Upper mantle attenuation and velocity structure from measurements of differential S phases. *Geophysical Journal International* 145: 615–630.

Resovsky JS and Ritzwoller MH (1998) New and refined constraints on three-dimensional Earth structure from normal modes below 3mHz. *Journal of Geophysical Research* 103: 783–810.

Resovsky JS, Trampert J, and van der Hilst RD (2005) Error bars for the global seismic Q profile. *Earth and Planetary Science Letters* 230: 413–423.

Revenaugh J and Jordan TH (1989) A study of mantle layering beneath the western Pacific. *Journal of Geophysical Research* 94: 5787–5813.

Revenaugh J and Jordan TH (1991) Mantle layering from ScS reverberations. Part 2: The transition zone. *Journal of Geophysical Research* 96: 19763–19780.

Richards PG and Menke W (1983) The apparent attenuation of a scattering medium. *Bulletin of the Seismological Society of America* 73: 1005–1021.

Romanowicz B (1987) Multiplet-multiplet coupling due to lateral heterogeneity: Asymptotic effects on the amplitude and frequency of the Earth's normal modes. *Geophysical Journal of the Royal Astronomical Society* 90: 75–100.

Romanowicz B (1990) The upper mantle degree. Part 2: Constraints and inferences on attenuation tomography from global mantle wave measurements. *Journal of Geophysical Research* 95: 11051–110710.

Romanowicz B (1994a) On the measurement of anelastic attenuation using amplitudes of low-frequency surface waves. *Physics of the Earth and Planetary Interiors* 84: 179–191.

Romanowicz B (1994b) Anelastic tomography: A new perspective on upper-mantle thermal structure. *Earth and Planetary Science Letters* 128: 113–121.

Romanowicz B (1995) A global tomographic model of shear attenuation in the upper mantle. *Journal of Geophysical Research* 100: 12375–12394.

Romanowicz B (1998) Attenuation tomography of the earths mantle: A review of current status. *Pure and Applied Geophysics* 153: 257–272.

Romanowicz B (2002) Inversion of surface waves: A review. In: Lee WHK (ed.) *Handbook of Earthquake and Engineering Seismology*, *IASPEI*, Part A, pp. 149–174. Amsterdam: Academic Press.

Romanowicz B and Durek J (2000) Seismological constraints on attenuation in the Earth: A review. In: Karato S-I, Forte AM, Liebermann RC, Masters G, and Stixrude L (eds.) *Geophysical Monograph Series* 117: *Earth's Deep Interior: Mineral Physics and Tomography from the Atomic to the Global Scale.* pp. 161–180. Washington, DC: American Geophysical Union.

Romanowicz B and Gung Y (2002) Superplumes from the core–mantle boundary to the lithosphere: Implications for heat-flux. *Science* 296: 513–516.

Romanowicz B, Roult G, and Kohl T (1987) The upper mantle degree two pattern: Constraints from Geoscope fundamental spheroidal model eigenfrequency and attenuation measurements. *Geophysical Research Letters* 14: 1219–1222.

Rosat S, Sato T, Imanishi Y, *et al.* (2005) High resolution analysis of the gravest seismic normal modes after the 2005 Mw = 9 Sumatra earthquake using superconducting gravimeter data. *Geophysical Research Letters* 32, doi:10.1029/2005GL023,128.

Roth E, Wiens DA, Dorman LM, Hildebrand J, and Webb SC (1999) Seismic attenuation tomography of the Tonga-Fiji region using phase pair methods. *Journal of Geophysical Research* 104: 4795–4809.

Roth E, Wiens DA, and Zhao D (2000) An empirical relationship between seismic attenuation and velocity anomalies in the upper mantle. *Geophysical Research Letters* 27: 601–604.

Roult G (1975) Attenuation of seismic waves of very low frequency. *Physics of the Earth and Planetary Interiors* 10: 159–166.

Roult G (1982) The effect of young oceanic regions on the periods and damping of free oscillation of the Earth. *Journal of Geophysical Research* 51: 38–43.

Roult G and Clévédé E (2000) New refinements in attenuation measurements from free oscillations and surface wave observations. *Physics of the Earth and Planetary Interiors* 121: 1–37.

Roult G, Romanowicz B, and Montagner JP (1984) 3D upper mantle shear velocity and attenuation from fundamental mode free oscillation data. *Geophysical Journal International* 101: 61–80.

Roult G, Rosat S, Clévédé E, Millot-Langet R, and Hinderer J (2006) New determination of Q quality factors eigenfrequencies for the whole set of singlets of Earth's normal modes ${}_0S_0$,${}_0S_2$, ${}_0S_3$ *and* ${}_2S_1$, using Superconducting Gravimeer data from the GGP network. *Journal of Geodynamcis* 41: 345–357.

Sacks IS (1969) Anelasticity of the inner core. *Annual Report of the Director of Department of Terrestrial Magnetism* 69: 416–419.

Sacks IS (1980) Qs of the lower mantle – A body wave determination. *Annual Report of the Director of Department of Terrestrial Magnetism* 79: 508–512.

Sailor RV and Dziewonski AM (1978) Measurements and interpretation of normal mode attenuation. *Geophysical Journal of the Royal Astronomical Society* 53: 559–581.

Sarker G and Abers GA (1998) Comparison of seismic body wave and coda wave measures of *Q*. *Pure and Applied Geophysics* 153: 665–683.

Sarker G and Abers GA (1999) Lithospheric temperature estimates from seismic attenuation across range fronts in southern and central Eurasia. *Geology* 27: 427–430.

Sato H, Sacks IS, Murase T, Muncill G, and Fukuyama F (1989) Qp-melting temperature relation in peridotite at high pressure and temperature: Attenuation mechanism and implications for the mechanical properties of the upper mantle. *Journal of Geophysical Research* 94: 10647–10661.

Sato R and Espinosa AF (1967) Dissipation in the Earth's mantle and rigidity and viscosity in the Earth's core determined from waves multiply-reflected from the mantle–core boundary. *Bulletin of the Seismological Society of America* 57: 829–856.

Schlotterbeck BA and Abers GA (2001) Three-dimensional attenuation variations in Southern California. *Journal of Geophysical Research* 106: 30719–30735.

Selby ND and Woodhouse JH (2000) Controls on Rayleigh wave amplitudes: Attenuation and focusing. *Geophysical Journal International* 142: 933–940.

Selby ND and Woodhouse JH (2002) The Q structure of the upper mantle: Constraints from Rayleigh wave amplitudes. *Journal of Geophysical Research* 107, doi:10.1029/20,001JB000,257.

Shearer P (1994) Constraints on inner core anisotropy from PKP(DF) travel times. *Journal of Geophysical Research* 99: 19647–19659.

Sheehan A and Solomon SC (1992) Differential shear wave attenuation and its lateral variation in the north Atlantic region. *Journal of Geophysical Research* 97: 15339–15350.

Shi J, Kim WY, and Richards PG (1996) Variability of crustal attenuation in the Northeastern United States from *Lg* waves. *Journal of Geophysical Research* 101: 25231–25242.

Shito A, Karato S, and Park J (2004) Frequency dependence of Q in Earth's upper mantle inferred from continuous spectra of body waves. *Geophysical Research Letters* 31, doi:10.1029/2004GL019,582.

Shito A and Shibutan T (2003b) Anelastic structure of the upper mantle beneath the northern Philippine Sea. *Physics of the Earth and Planetary Interiors* 140: 319–329.

Shito A and Shibutan T (2003a) Anelastic structure of the upper mantle beneath the northern Philippine Sea. *Physics of the Earth and Planetary Interiors* 140: 319–329.

Singh S and Herrmann RB (1983) Regionalization of crustal Q in the continental United States. *Journal of Geophysical Research* 88: 527–538.

Singh SC, Taylor MJ, and Montagner JP (2000) On the presence of liquid in the Earth's inner core. *Science* 287: 2471–2474.

Sipkin SA and Jordan TH (1979) Frequency dependence of Q_{ScS}. *Bulletin of the Seismological Society of America* 69: 1055–1079.

Sipkin SA and Jordan TH (1980) Regional variation of QScS phases. *Bulletin of the Seismological Society of America* 70: 1071–1102.

Sipkin SA and Revenaugh J (1994) Regional variation of attenuation and travel times in China from analysis of multiple ScS phases. *Journal of Geophysical Research* 99: 2687–2699.

Smith S (1972) The anelasticity of the mantle. *Tectonophysics* 13: 601–622.

Smith ML and Dahlen FA (1981) The period and Q of the Chandler wobble. *Geophysical Journal of the Royal Astronomical Society* 64: 223–282.

Smith MF and Masters G (1989) Aspherical structure constraints from free oscillation frequency and attenuation measurements. *Journal of Geophysical Research* 94: 1953–1976.

Sobolev SV, Zeyen H, Soll G, Werling F, Altherr R, and Fuchs K (1996) Upper mantle temperatures from teleseismic tomography of French Massif Central including the effects of composition, mineral reactions, anharmonicity, anelasticity and partial melt. *Earth and Planetary Science Letters* 139: 147–163.

Solomon SC (1973) Seismic wave attenuation and melting beneath the Mid-Atlantic Ridge. *Journal of Geophysical Research* 78: 6044–6059.

Song XD and Helmberger D (1993) Anisotropy of the Earth's inner core. *Geophysical Research Letters* 20: 285–288.

Souriau A and Romanowicz B (1996) Anisotropy in inner core attenuation: A new type of data to constrain the nature of the solid core. *Geophysical Research Letters* 23: 1–4.

Souriau A and Romanowicz B (1997) Anisotropy in the inner core: Relation between P-velocity and attenuation. *Physics of the Earth and Planetary Interiors* 101: 33–47.

Souriau A and Roudil P (1995) Attenuation in the uppermost inner core from broadband GEOSCOPE PKP data. *Geophysical Journal International* 123: 572–587.

Street RL (1976) Scaling Northeastern United States/ southeastern Canadian earthquakes by the *Lg* waves. *Bulletin of the Seismological Society of America* 66: 1525–1537.

Strick E (1967) The determination of Q, dynamic viscosity and creep curves from wave propagation measurements. *Geophysical Journal of the Royal Astronomical Society* 13: 197–218.

Su WJ and Dziewonski AM (1990) Inner core anisotropy in three dimensions. *Journal of Geophysical Research* 100: 9831–9852.

Suda N and Fukao Y (1990) Structure of the inner core inferred from observations of seismic core modes. *Geophysical Journal International* 103: 403–413.

Suda N, Nawa K, and Fukao Y (1998) Earth's background free oscillations. *Science* 279: 2089–2091.

Suda N, Shibata N, and Fukao Y (1991) Degree 2 pattern of attenuation structure in the upper mantle from apparent complex frequency measurements of fundamental spheroidal modes. *Geophysical Research Letters* 18: 1119–1122.

Suetsugu D (2001) A low Q_{ScS} anomaly near the South Pacific Superswell. *Geophysical Research Letters* 28: 391–394.

Sumita I and Olson P (1999) A laboratory model for convection in Earth's core driven by a thermally heterogeneous mantle. *Geophysical Research Letters* 286: 1547–1549.

Sutton GH, Mitronovas W, and Pomeroy PW (1967) Short-period seismic energy radiation patterns from underground explosions and small-magnitude earthquakes. *Bulletin of the Seismological Society of America* 57: 249–267.

Tanaka S and Hamaguchi H (1997) Degree one heterogeneity and hemispherical variation of anisotropy in the inner core from PKP(BC)-PKP(DF) times. *Journal of Geophysical Research* 102: 2925–2938.

Teng TL (1968) Attenuation of body waves and the Q structure of the mantle. *Journal of Geophysical Research* 73: 2195–2208.

Thouvenot F (1983) Frequency dependence of the quality factor in the upper crust: A deep seismic sounding approach. *Geophysical Journal of the Royal Astronomical Society* 73: 427–447.

Trampert J and Woodhouse JH (1995) Global phase velocity maps of Love and Rayleigh waves between 40 and 150 seconds. *Geophysical Journal International* 122: 675–690.

Tryggvason E (1965) Dissipation of Rayleigh-wave energy. *Journal of Geophysical Research* 70: 1449–1455.

Tsai YB and Aki K (1969) Simultaneous determination of the seismic moment and attenuation of seismic surface waves. *Bulletin of the Seismological Society of America* 59: 275–287.

Tseng TL, Huang BS, and Chin BH (2001) Depth-dependent attenuation in the uppermost inner core from the Taiwan short period PKP data. *Geophysical Research Letters* 28: 459–462.

Ulug A and Berckhemer G (1984) Frequency dependence of Q for seismic body waves in the Earth's mantle. *Journal of Geophysics* 56: 9–19.

Utsu T (1967) Anomalies in seismic wave velocity and attenuation associated with a deep earthquake zone. *Journal of the Faculty of Science, Hokkaido University* 7: 1–25.

Vidale JE and Earle PS (2000) Fine-scale heterogeneity in the Earth's inner core. *Nature* 404: 273–275.

Vinnik LP, Romanowicz B, and Bréger L (1994) Anisotropy in the center of the Inner Core. *Geophysical Research Letters* 21: 1671–1674.

Warren LM and Shearer PM (2002) Mapping lateral variation in upper mantle attenuation by stacking *P* and *PP* spectra. *Journal of Geophysical Research* 107, doi:10.1029/ 2001JB001,195.

Wen L and Niu F (2002) Seismic velocity and attenuation structures in the top of the Earth's inner core. *Journal of Geophysical Research* 107, doi:10.1029/2001JB000,170.

Widmer R, Masters G, and Gilbert F (1991) Spherically symmetric attenuation within the Earth from normal mode data. *Geophysical Journal International* 104: 541–553.

Wilcock WSD, Solomon SC, Purdy GM, and Toomey D-R (1995) Seismic attenuation structure of the East Pacific Rise near 9° 30m N. *Journal of Geophysical Research* 100: 24147–24165.

Wong YK (1989) *Upper Mantle Heterogeneity from Phase and Amplitude Data of Mantle Waves*. PhD Dissertation, Harvard University, Cambridge, MA.

Woodhouse JH and Wong YK (1986) Amplitude, phase and path anomalies of mantle waves. *Geophysical Journal of the Royal Astronomical Society* 87: 753–773.

Xie J, Gok R, Ni J, and Aoki Y (2004) Lateral variations of crustal seismic attenuation along the INDEPTH profiles in Tibet from *LgQ* inversion. *Journal of Geophysical Research* 109(B10): 308 (doi:10.1029/2004JB002,988).

Xie J and Mitchell BJ (1990a) Attenuation of multiphase surface waves in the Basin and Range province. Part I : *Lg* and *Lg* coda. *Geophysical Journal International* 102: 121–127.

Xie J and Mitchell BJ (1990b) A back-projection method for imaging large-scale lateral variations of *Lg* coda *Q* with application to continental Africa. *Geophysical Journal International* 100: 161–181.

Xie J and Nuttli OW (1988) Interpretation of high-frequency coda at large distances: Stochastic modeling and method of inversion. *Geophysical Journal* 95: 579–595.

Xie J, Wu X, Liu R, Schaff D, Liu Y, and Liang J (2006) Tomographic regionalization of crustal *Lg Q* in eastern Eurasia. *Geophysical Research Letters* 33(L03): 315 (doi:10.1029/2005GL024,410).

Yacoub NK and Mitchell BJ (1977) Attenuation of Rayleigh wave amplitudes across Eurasia. *Bulletin of the Seismological Society of America* 67: 751–769.

Yoshida M and Tsujiura M (1975) Spectrum and attenuation of multiply-reflected core phases. *Journal of Physics of the Earth* 23: 31–42.

Yu W and Wen L (2006) Seismic velocity and attenuation structures in the top 400 km of the Earth's inner core along equatorial paths. *Journal of Geophysical Research* 111: (doi:10.1029/2005JB003,995).

Zhang T and Lay T (1994) Analysis of short-period regional phase path effects associated with topography in Eurasia. *Bulletin of the Seismological Society of America* 84: 119–132.

Relevant Website

http://mahi.ucsd.edu – The Reference Earth Model